People's Democratic Republic of Algeria

Ministry of Higher Education and Scientific Research

University M'Hamed BOUGARA – Boumerdès

Institute of Electrical and Electronic Engineering

Department of Control and Power

Final Year Project Report Presented in Partial Fulfilment of
The Requirements of the Degree of

'MASTER'

In **Control**

Option: **Control**

Title:

Detection and Diagnosis of PV system faults.

Presented By:

- **BOUDJADAR Mohamed Mounib**

Supervisor:

Dr. KHELDOUN Aissa.

Registration Number:...../2018

DEDICATION

I would like to dedicate this modest work to my beloved parents and my family. To all my friends and colleagues who have helped me along the way.

ACKNOWLEDGMENT

In the beginning, I thank Allah for his blessings upon us, for giving me the strength and guidance to accomplish this project.

I would like to extend my gratitude to my supervisor Dr. **A.Kheldoun** for his advice and assistance in the order of finishing this work.

I also, would like to express my thanks to all the people who have been of help to myself during the period of this project.

ABSTRACT

The photovoltaic systems are gaining more importance as reliable energy producing systems, due to the fact of that the solar energy is green and renewable. In spite of the instability of electricity generation and the low efficiency, the PV systems have relatively long life span. Similar to any other system, the PVS endure losses and are exposed to failures with different significance. Hence a diagnosis system is required to monitor and detect the faults' existence. This project concern is developing a fault diagnosis system with the purpose of identifying the occurrence of the most common faults in a PV system based on the current and voltage assessment under different conditions.

Table of Contents

List of Figures

List of Tables

Nomenclature

T	**Temperature**
G	**Irradiance**
I_{mpp}	**Current at the maximum power point**
V_{mpp}	**voltage at the maximum power point**
Isc	**Short-circuit current**
V_{oc}	**Open-circuit voltage**
V_t	**Thermal voltage**
K	**Boltzmann constant, $K=1.38*10^{-23}$ J/°K**
q	**Electron charge $q=1.602*10^{-19}$ C**
A	**ideality factor**
I_{ph}	**photo-current of the solar cell**
I_0	**diode saturation current.**
Rs	**Series resistor of solar cell equivalent model**
Rsh	**Shunt resistor of solar cell equivalent model**
U_c	**Current indicator**
Uc_r	**Current indicator in normal operation**
U_v	**Voltage indicator**
U_{v_r}	**Voltage indicator in normal operation**
Ns	**Number of module in series**
N_p	**Number of modules in parallel**

List of Acronyms

STC	**Standard Test Conditions**
PV	**Photovoltaic**
MPPT	**Maximum Power point tracking**
AI	**Artificial intelligence**
ANN	**Artificial Neural Network**
PWM	**Pulse Width Modulation**

GENERAL INTRODUCTION

Since the last century, the dependence of the humans on the fossil sources of energy kept growing along with the technological development, governing a huge part of the world's economy till the present, which will not be the case in few decades as these sources are limited expensive and non-renewable. In contrast to the renewable energies, they are causing a disagreeable and dangerous effect on the environment.

The renewable energies such as the wind and solar energy, are the path toward a cleaner world as well as compensating the rapidly increasing demand.

The daily availability of sunlight makes the solar energy an enormous green source for the individual use or the industrial purposes. Divided into two types: the thermo and the photovoltaic based conversion of the sunlight into electricity. The modern available blocks of the energy harvesting system use the latter. Coming a long way of development, the current photovoltaic systems are available at reasonable costs, especially with the implementation of photovoltaic systems connected to the grid utility, reducing both the fees and peak needs. The remote locations where the grid is unavailable or far, installing a solar system is very useful and cost-effective.

Another advantage of the solar energy is reducing the need for the supplied by the grid power.

Increasing the efficiency of the photovoltaic systems has been the essential research and development subject. Furthermore, the instability of the conditions under which the energy is generated requires some parameters variation as well as the need for the production monitoring. This task is meant to supervise the well operation of the system in light of the several faults that may affect the system's component by reason of degradation or lack of performance, causing energy losses and efficiency reduction or even permanent damage to the system. In parallel with monitoring, the diagnosis of an abnormal behavior of the system and determining its causes and results is very crucial. In order to perform this diagnosis, the literature survey shows that numerous methods have been developed to execute this continuous operation. Falling into two major groups differing by the use of a system's model to identify the normal and faulty behavior based on comparison and error evaluating. The other group consists of the artificial intelligence based methods, which are most needed where the system's model could not describe both the healthy and faulty operation accurately.

This thesis is divided into four chapters.

The first chapter provides a state of the art about the monitoring and the fault diagnosis systems, and the common methods adopted for the PV system's fault diagnosis. The second chapter gives a general overview of the photovoltaic system and its main components, along with a theoretical elaboration about the light-generated electricity and its characteristics. As for the third chapter, it represents the modeling of PV system's the DC part, and the configuration chosen in the model, as well as modeling some of the faults. The last chapter contains the fault indicators used to detect the faults selected, and the system's response to them, besides the validation of the method by taking several test cases. Finally, the general conclusion summarizes the work done in the thesis, and opens a tab for future works discussion.

CHAPTER 1 : STATE OF THE ART

1.1 Introduction:

Solar power plants are considered reliable systems for power generation [2]. However, they are affected by several types that would affect the normal functioning of the system, and thus affect the production. When the system generates less power than expected, it is considered as an abnormal behavior for which the cause would be interpreted as a fault.

As the system has several components, different types of faults may occur during the system's operation, either controllers' software or components' hardware, for various reasons.

However, by analyzing different measurements we can distinguish the type of the system's malfunction and the reason causing it.

1.2 Common PV system faults

In order to categorize the faults, it would be more efficient to divide the system into two main parts, the first being the DC side, and the second is the AC side including the grid-connection and the DC-AC inverter.

At the moment, the sold inverters have their own fault detection system implemented within, to distinguish almost all possible failures and displays the error.

Some of the faults on AC side of the system are:

- Inverter heating: which could be caused by lack of ventilation in high temperatures.
- The disparity between the grid's frequency and the inverter's output's frequency.
- Instability of the grid feedback compensation when there is low yield.

The DC side includes two subsections of its own, the PV array and DC-DC converter. The PV array's most common faults are:

- Short-circuit faults: including all short-circuited cells, modules, bypass diodes, or any other connection wire. It also could be caused by humidity.
- Open-circuit faults: which could be caused by malfunction of blocking diodes, cells deterioration or breakdown.
- Reversed polarity when installing, either of diodes or PV modules wiring.

- Shunt resistance: which could be created parallel to the PV modules or the bypass diodes, due to corrosion or aging. [4]

In addition to these, the whole PV system could have faults caused by bad wiring and loose connections in any part of the system. Although the system's life span is long, aging has its effect on all the components causing efficiency decrease, and so does the corrosion.

- **Partial shading:**

Caused when the array is exposed to non-uniform irradiance, due to outsider obstacles, trees, clouds, and also due to snow settling on top of the array as well as sand's and dirt's accumulation. When a sub-array (one module or more) has lower incident irradiance, it starts acting like a sink that absorbs power from the other unshaded modules connected in series with it, with the shaded module has a reverse biased state and the current is forced on the module which would damage it.

For avoiding this problem a bypass diode is installed parallel to each one or couple of modules. In normal operation, this bypass diode is reverse biased, when the module is shaded, it the voltage drop makes the diode forward biased which will be short-circuiting the shaded module for the objective of protecting it.

The partial shading phenomenon causes the PV array power losses and affect its normal operation, it may create several power peaks. [5]

- **MPP tracking error**

Resulting loss of power and efficiency of the system, the tracking error could be caused by defection of the controller, communication fault or a measurement fault, as well as the issue being a DC-DC converter failure originated by components degradation or faulty wiring.

1.3 Monitoring systems:

Monitoring is a continuous real-time operation of determining the possible conditions of a system, recognizing and indicating anomalies in its behavior [6]. System's monitoring is very important task in order to know how the PV system is performing under all circumstances.

The first step is recovering the data from the PV system, through the measurement system with the hardware (sensors) already incorporated in the plant installation by the manufacturer, and the inverter's data as well. The information is acquired through either computers or data-logger boards depending on the customization desired for the system

and the cost assessment. The data collected is displayed to supervision, and set as inputs to the next step of the monitoring being the evaluation of this data [2,3].
The table 3.1 shows the typical accuracy for the monitoring systems [7].

Table 12-1-1 Monitoring system's accuracy.

Parameter	Sensor	Accuracy
Solar irradiance	Pyranometer or reference cell	2%
DC current	DC-DC converter or the DC-AC inverter	1%
AC current	The inverter	1%
Ambient temperature	Thermocouple	1C°
	PRT	0.2 C°
Power	AC meter	1%

Evaluating the data collected is done by evaluating the performance parameters such as array yield, final yield and performance ratio, after being calculated as a function of the measurements. Most of PV companies use the performance ratio (PR) as an indicator of the operating condition of the PV plant [2]. The objective is to give an accurate feedback about system's operating condition under different circumstances, and give the ability to assess the fault occurrence possibility.

1.4 Fault detection & diagnosis

For the purpose of ensuring reliability of the power production operation of the PV system and the optimization of the energy harvesting process in a fault free conditions, the fault diagnosis is performed continuously, which as well enable the maintenance operation in more time and cost effective manner in case of failures and anomalous behavior. Moreover, to assess the different losses taking place in all levels of the system, such as losses caused by component degradations, shading or control signals error. [8]

Various approaches are available for the PV system monitoring, based on the current, voltage levels, with respect to the measured irradiance and temperature.

Having different efficiencies and properties, the criteria about which the differences between them are laid, are mainly:

- The ability of detection of numerous faults, novel or known ones.

- The ability to distinguish dissimilar faults with similar symptoms.
- The robustness of the system toward noise and model errors.
- The response time of the diagnosis system after a fault occurrence.
- The system's ability to identify the fault source and impact on the performance.
- The diagnosis system's implementation cost either for software hardware required. [3]

1.4.1 Fault diagnosis methods:

In order to effectuate the fault diagnosis in the PV array, we can split the common methods into two distinct categories:

1.4.1.1 Non-electric methods:

Several non-electric methods are adopted with the aim of determining the occurring of faults, among which, there is the infrared imaging.

a. Infrared imaging:

Since the operating temperature of a PV cell or module varies, the changes in case of abnormal operation can be observed with contrast to other healthy modules. Using the infrared imaging, the location of the deteriorated or defective module is precisely determined in a thermal image of the system [20].

1.4.1.2 Electrical methods

a. Methods based on analyzing the IV characteristics

Several fault detection methods are based on analyzing the parameters of the IV characteristics of the PV array. A faulty array has discrepancies in its voltage and current features, resulting the reduction of the maximum power generated. Among the methods we have:

❖ **Method based on analyzing IV symptoms**

The first step of this method is establishing a knowledge basis of the system's behavior under a faulty state. In order to pursue that, numerous fault scenarios are studied for different parts of the system (sub-arrays, strings, modules), under different operating conditions of temperature and irradiance.

Examining the result of each simulation carried, behavioral symptoms are obtained for the fault simulated which will allow the future recognition of the fault's causes when the same symptom is observed during the system's operation. The fault indicators are based on the analysis of the maximum power losses, open-circuit voltage

and short-circuit current. Moreover, the presence of an inflection point or more than one MPP. This methods allows to identify some of the faults mentioned before, but lacks the ability to localize exactly the faulty component every time, when similar faults are present in different parts of the system [9,3].

❖ **Method based on (-dI/dV—V) characteristics curve:**

If we consider the value dI/dV, it is the slope of the I-V characteristics curve, it is described by an increasing magnitude and a negative sign as the voltage increases. However, in case of partial shading, the array's characteristics change, and I-V curve suffers inflection points corresponding to more than one power peaks in the P-V curve. At the inflection points, the "-dI/dV -V" has a local maximum. The corresponding voltage value varies with the number of shaded modules, more shaded ones pushes the peak towards the left reducing the voltage more significantly and vice versa [21].

b. Method based on analyzing power and energy yields:

The system endures losses of various nature, constant such as soiling and component degradation or variable such as shading or MPP tracking [2], to acknowledge these abnormal conditions by performing this diagnosis method, different fault indicators can be evaluated continuously. The indicators could be array yield, reference yield, performance ratio or maximum power point tracking [14], among several others.

Calculated from the measurements, the monitored data is compared with the model simulated data, with the healthy state of the system is made reference, and fault residuals are generated when the error magnitude exceeds the tolerance levels.

1.4.1.3 Artificial intelligence based methods:

Several AI methods have been used for implementing a fault diagnosis system, all based on the data-driven algorithm where typically a collection of measurements representing different instances of the system's operation is available [25]. Moreover, they are characterized by the learning ability which is achieved given training data. The AI provides a powerful tool in performing the fault diagnosis, due to the ability to identify novel inconsistencies in the system's operation based on its data. Among these methods, the fuzzy logic and the neural networks are commonly used.

a. Artificial neural networks (ANN) based method:

In order to build up an ANN, the inputs and outputs of the neural network have to be defined for pattern recognition. Inputs to the network should provide a true representation

of the situation under consideration [26]. For a PV array case, the MPP coordinates, the irradiance and temperature are taken as inputs to multi-layers ANN, where the output sought is the voltage and current of each PV module in the array, and which are inputs to the alarm system, so does the error between the estimated and actual outputs [27].

b. Fuzzy logic based method:

Fuzzy models as a nonlinear black box-structure represent the relationships between past observations [u(t-1); y(t-1)] and the future outputs y(t) of a general discrete time dynamic system:

$$y(t) = g\big(u(t-1), y(t-1)\big) + v(t)$$

The additive term v(t) accounts for the fact that the next output y(t) will not be an exact function of past data.[25]. This method is able to identify several faults, such as, the series resistance increase and the partial shading.

1.5 Conclusion:

In this chapter, some of the common faults present in the PV system are mentioned and briefly elaborated. The monitoring and the fault diagnosis methods, dissimilar in properties, requirements and response, also dissimilar in inputs and the types of faults that could be identified accurately, are grouped into three main categories, electric, non-electric and artificial intelligence based.

Prior to implementing a diagnosis system, a system's model is laid and its configuration is chosen, which is done in the next chapter.

CHAPTER 2 : PV SYSTEM OVERVIEW

2.1 Introduction:

The Photovoltaic system design consists of several blocks, taking the sunlight as the source and producing DC or AC electricity, upon requirements. The first and main part is the PV array which represent the core of the operation, after which, comes the DC-DC converter, which is considered the first level of adaptation. Unless the PV system is designed to feed a DC load, it is occupied with another block called the inverter, converting the DC generated power into an AC one, to be delivered to an AC load or to the grid utility.

In order to produce solar-generated electricity, a photovoltaic system has solar cells as the corner stone. So, for the purpose of better understanding the system's function we start by introducing the solar cell.

2.2 The solar cell:

A solar cell is an electric device which has the property of converting the energy provided by the photons in sun light into electrical potential and current. This semi-conductor device make this phenomenon happen under the effect known as the photovoltaic effect, in other words, turn light into electricity. The figure 2-1 shows a solar cell circuit and a simple illustration of the light-generated current creation.

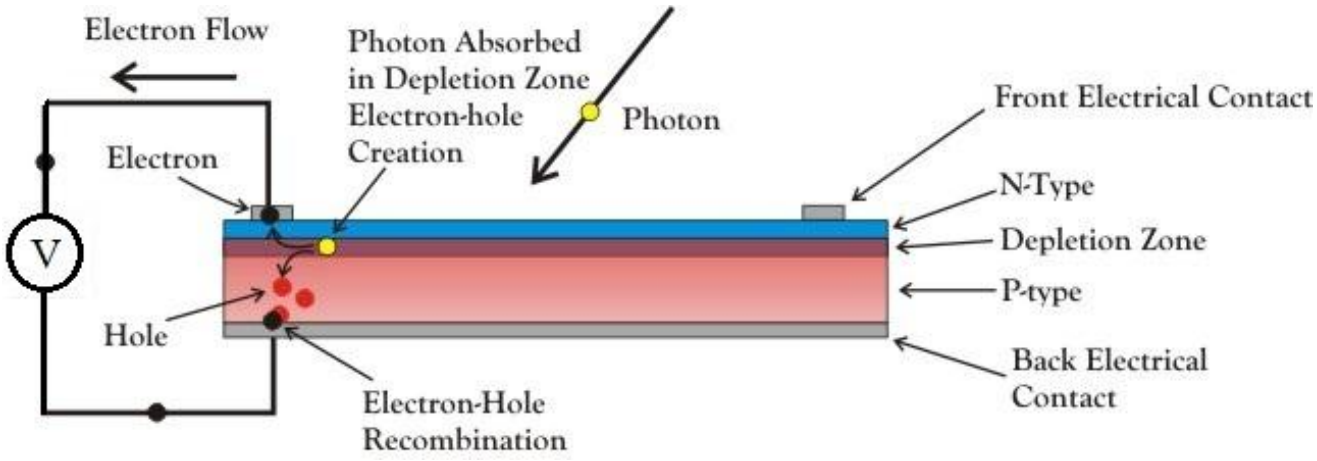

Figure 3-2-1 A solar cell schematic

2.2.1 The photovoltaic effect:

The photovoltaic effect was first discovered in 1839 by Edmond Becquerel. When the light is shed upon the solar cell, the electrons on the valence band absorb enough energy to be excited and jump to the conduction band, an electron-hole pair is then created in the PN-junction, those pairs create an electric potential, inducing an electromotive force, therefore each solar cell produce electricity, with a voltage and a current that are dependent on the level of exposure to solar irradiance, and the ambient temperature in which the solar cell is sited. [1]

2.3 The PV array:

As the name suggests, a PV array consists of several PV modules both in series and parallel, connected in different topologies, depending on the number of modules used, as well as the levels of voltage and current desired at the output of the array.

Each and every one of those modules is made of another alignment of solar cells, which are the corner stone of the solar energy.

Inside the array, a group of PV modules connected in series is called a “string”. Each string is protected at the end by a blocking diode for the purpose of module’s protection. Whereas each module or couple of modules have a bypass diode connected in parallel with them.

2.3.1 The blocking diode

Installed in series with the PV modules in a string, the purpose of the blocking diode is the protection of the PV modules from the reverse current. It prevents the current from flowing down the modules in case of flow back from the battery or the load. Moreover, in case of a defective module or a severely shaded string, it prevents the other modules from losing the generated current forced backward down the damaged string, in other words, isolate it. [19].

2.4 dc-dc chopper

The output of the PV array is not a constant signal but a function of other variables, it has an operating point that varies continuously with the variation of the irradiance and the ambient temperature, and we need to extract the point of maximum power of operation, for that an MPPT algorithm, based on PWM modulation is implemented on the first of two levels of the conversion process.

The other task of the chopper is to produce a stable voltage and current which will be converted into an Ac one. The DC converter could be a buck or boost converter

depending on the design of the system. It, also, could be implemented as a buck-boost model, which is the most common of cases.

2.5 The DC-AC inverter

At this level, we have a DC signal, and whether the purpose is to supply it to the grid or to a stand-alone isolated usage, we need to have an alternative current, therefore we need to actuate a DC-AC conversion.

Beside generating the ac current, and in order for the electricity produced to match the grid's both frequency and amplitude, the inverter takes care of this task by varying the duty cycle on the IGBT switches to output a proper sine wave with the right amplitude and frequency.

2.6 Electrical characteristics

Based on the material and the manufacturing process, each solar cell has a nominal current voltage relationship characteristic. Where the elementary parameters of the PV modules composed of those cells are determined by the manufacturer in the datasheet of the PV module, at the STC (Standard Testing Conditions G= 1000, T=25 °). This characteristic relationship is well interpreted in the predetermined I-V curve which is typically similar to Figure 2-2.

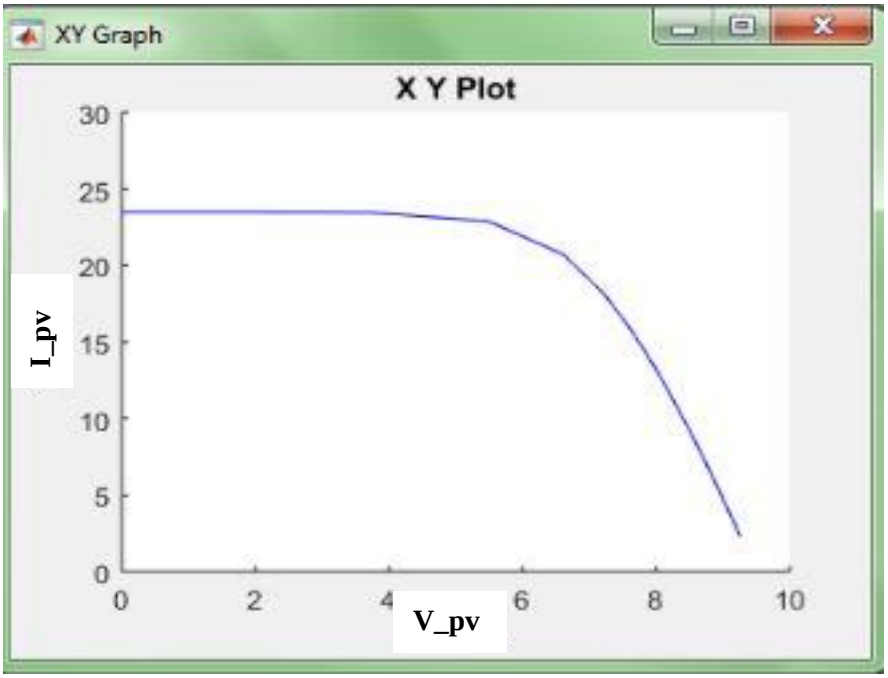

Figure 2-2 I-V characteristics curve for a PV module

2.6.1 The IV curve

The operating point of the solar cell is a function of the load connected to the cell's output. It varies along the IV curve. When light is shed upon an unloaded cell, the voltage build up in the PN junction of the solar cell of approximately 0.6 volts is called "the open-circuit" voltage $\mathbf{V_{oc}}$. It also is the maximum voltage a solar cell can produce. On the other hand, when the two terminals of the solar cell are short-circuited, the voltage is virtually null, however the current measured is at its maximum value, and called the short-circuit current **Isc**. [2]. In figure 2-2, this variation is shown for a single PV module with 4 parallel strings, of which, each consist of 16 series cell each.

The changes in irradiance and temperature affect the behavior of the system, scaling the characteristics curves, and changing the operating point, i.e. changing the output voltage and current and hence the power.

2.6.2 Scaling the IV curve

Each string in the PV array, having several modules connected in series, will have a voltage being the aggregate of each module's voltage, while keeping the same current ideally. This addition will be scaling the IV curve to the right along the x-axis (voltage axis).

No matter what the array topology is, it has a number of strings connected in parallel, this will add up the array's output current and scales the IV-curve up.

The following figure 2-3 displays a clear interpretation of the IV scaling with respect to the number of modules connected in parallel (Np), and series (Ns).

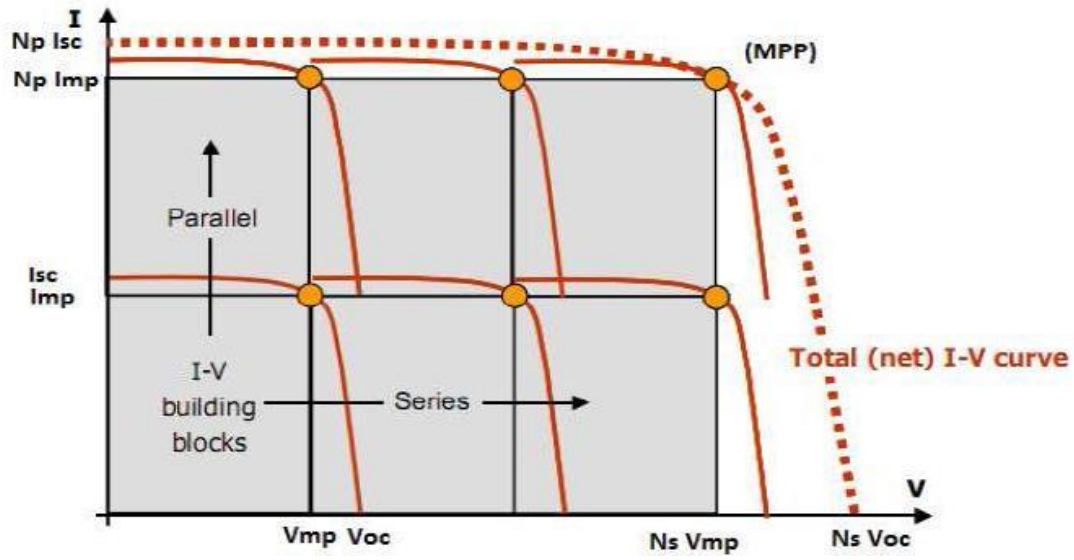

Figure 2-3 IV curve scaling in a PV array

The series and parallel connection topology of the modules varies from one panel to another, based on the nominal voltage and current sought from the array, which is chose upon the purpose of usage it is designed for.

2.6.3 Effect of temperature and irradiance on the IV curve:

As mentioned before, the power generated by the PV system is directly and strongly affected by the climatic changes, precisely, the irradiance levels and the ambient temperature.

As clearly reflected in the figure, the current is widely reduced by the change of irradiance, in a directly proportional way, where the former drops to half when the latter does. However, the open-circuit and the MPP voltage are only changed slightly (10% change for 80% change in irradiance). Both the current and the voltage are then functions of irradiance, with coefficients determined by the manufacturer in the datasheet.

On the other hand, the cell's voltage is affected mostly by the ambient temperature. These changes determines the system voltage range and therefore the design of the entire PV system. Although, the temperature's changes influence the IV characteristics curve differently but it would change the operating point of the PV array, and therefore the energy yielded. The figure 2-4 shows the characteristics' curve changes with irradiance and the temperature variation for five different values of both [2].

This change in the voltage and current is ideally governed by the equations mentioned in the next chapter.

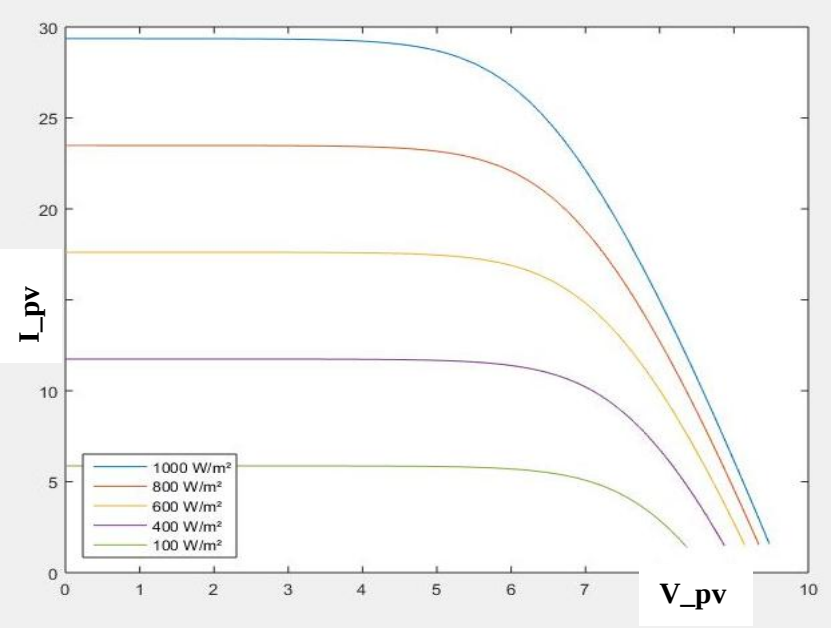

Figure 2-4 Irradiance effect on the IV characteristics curve

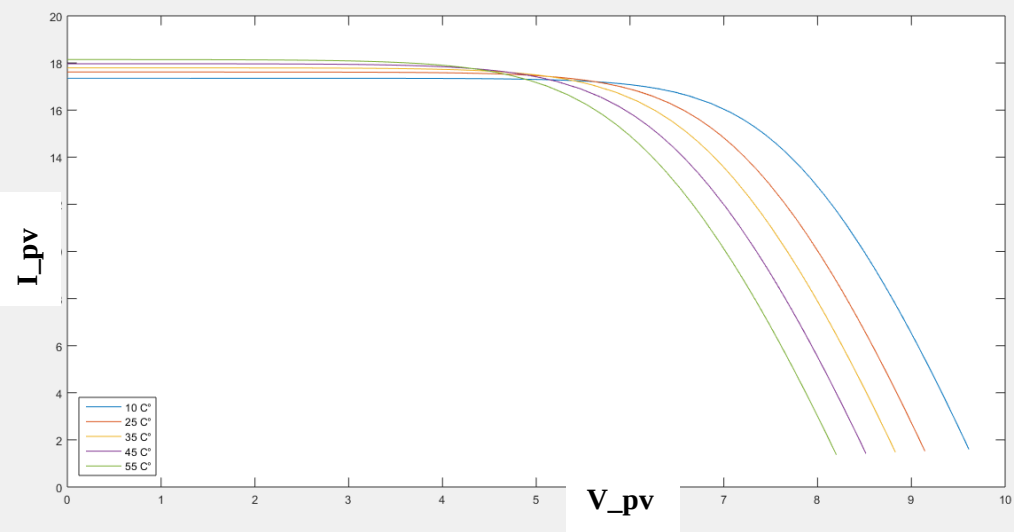

Figure 2-5 Temperature effect on the IV characteristics curve

2.6.4 Power curve

As we notice in the PV curve in the next figure, the output power of the PV array has a maximum point, this point correspond to the two coordinates $I=I_m$ and $V= V_m$ on the IV curve. In order to operate the system in maximum efficiency, we need to keep the system functioning as close as possible to that point, knowing that it varies continuously with the irradiance and temperature changes and the system's components' conditions.

For this purpose, we need to implement a maximum power point tracking algorithm which will allow us to reach the maximum efficiency of our PV array.

Since the load's variation changes the current, voltage and hence the power rates, the MPPT algorithm would be implemented in the next block of the system being the DC-DC converter, the power point tracking is done by the variation of the conversion rate.

The figure 2.6 shows the PV curve as the load varies from short to open circuit. The the maximum power point is appointed on the figure 2.6-a for both P-V and I-V curves.

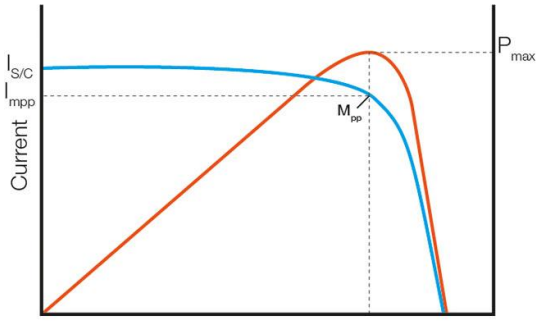

Figure 2-6-a- IV and PV curve

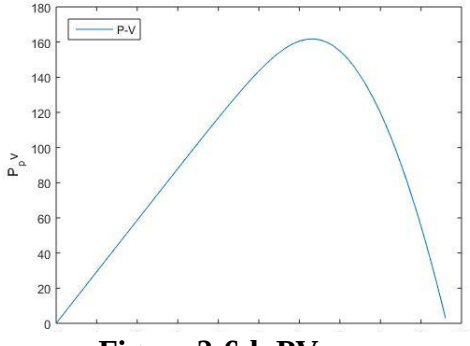

Figure 2-6-b PV curve

2.7 Photovoltaic systems configurations

Based on how the PV system is connected, we can distinguish two groups, a stand-alone and a grid-connected systems.

2.7.1 Stand-alone systems

In spite of the growing interest and research in the other group, the stand-alone PV systems are the most popular systems used worldwide, especially where the grid electricity was not available or not cost-effective, in relatively remote areas, or in mobile systems, such as cars and solar pumps used mostly for agriculture. The electricity generated in this type of system is going directly for usage when there is a load, however since the load is varying, as well as the energy yielded by the PV system, usually a battery is connected to the PV array's output to store the electricity, where there is a charge controller to monitor the battery charging when there is more energy yielded by the array than needed by the load, and the battery supplying the load to compensate the lack when the array's energy is reduced below the load's demand or when there is absence of production (very low irradiance or at night). [2][3].

The figure 2.7 represent a simple stand-alone solar system

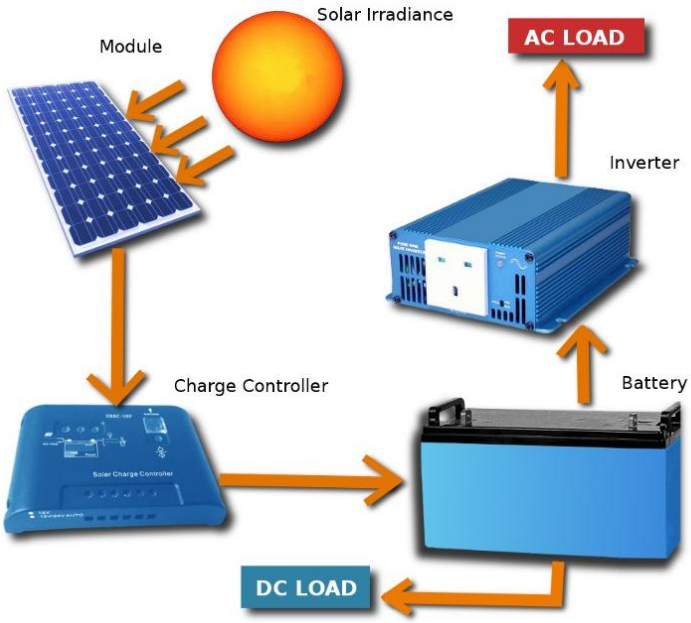

Figure 2-7 Stand-alone PV system

2.7.2 Grid-connected PV systems

This type of systems is becoming more popular lately, especially in the countries where the utility grid is available and the electricity cost is relatively high. Where the

stand-alone system is comparatively simpler, the grid connected system offers several advantages.

The fact that some of the electricity is produced from the PV system reduces the demand on the utility, which is important during peak hours.

Furthermore, some of the countries recently are using what's called the **net metering,** which is cost-reduction wise, when the PV system is yielding more electricity than needed, it supply the extra energy to the grid rather than let it go to waste, and the opposite happens when the yield is less than demanded. This means that all the energy produced by the system is benefited from, and the amount of grid's electricity one would have to pay for would be only the difference between the PV electricity supplied to the grid and the amount the latter supplies to the user.

The figure 2-8 shows the schematic of a grid connected PV system.

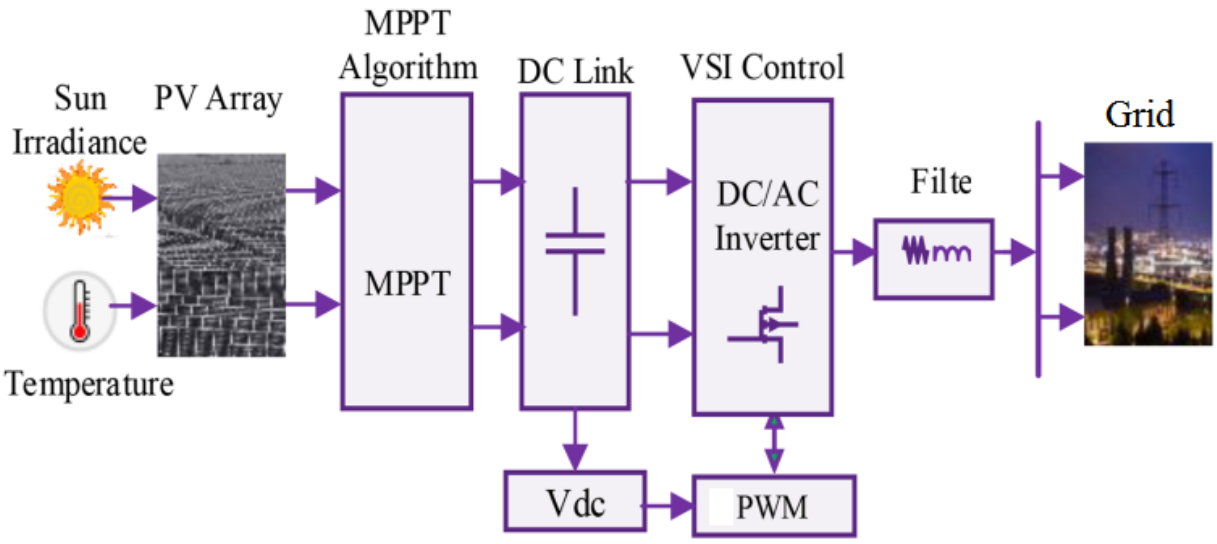

Figure 2-8 Schematics of a grid-connected PV system.

CHAPTER 3 : PV SYSTEM MODELING

3.1 Introduction

In order to study the system's behavior, and make the comparison between the healthy and the faulty operation state, a system's model is required to simulate the PV array's response, and evaluate its characteristics variations under different conditions. Former to build an array model, we have to choose a convenient single cell equivalent model, select its parameters according to existing solar cells, preserving the I-V characteristics for further use in building the whole system's model.

3.2 Solar cell model:

3.2.1 State of the art model:

For a purpose of representing the solar cell, various models have been proposed in the literature, falling in two categories, implicit and explicit models, these models differ mainly in the mathematical equations used to describe the behavior, as well as the parameters chosen to interpret the current-voltage relationship of the photovoltaic cell.

As the accuracy of the model varies, so does its simplicity, the simplest model consists of a current source of the light-generated current parallel to a diode, and a series resistor is added to represent the heat losses. A better approach is proposed, called the "single-diode model", where a shunt resistance is introduced, parallel to the diode for the purpose of expressing the internal losses of the cell under the variation of irradiance and temperature. [11][3]. Furthermore, a second diode could be introduced, to offer even more precision by considering the losses at the PN junction [18], however the model consist now of seven parameters rather than five with the single diode model, that echoes a trade-off between simplicity and accuracy especially when the temperature conditions are farther than the nominal value.

Explicit models are based on parameters that could be determined analytically, whereas implicit models parameters are not given by the manufacturer, and needed to be extracted, where two methods can be applied. The first is based on knowledge of the essential points of the I-V curve and an iterative process is applied, the iterations require initial values which if chosen properly, the convergence to the sufficiently precise values is fast, otherwise it could drive the results towards inconsistent results. The other method is the analytical approach to recover the exact parameters of the model, optimized by artificial intelligence algorithms. [3]

3.2.2 Single-diode model:

The single diode model consists of and ideal solar-induced current source, otherwise called the photocurrent (I_{ph}) a diode (D) and a shunt resistor (Rp) are in parallel with it, the latter describes the leakage current losses and has large value, in contrast of the resistor (Rs) which is in series with all the previous elements. This model is represented the figure. [12]

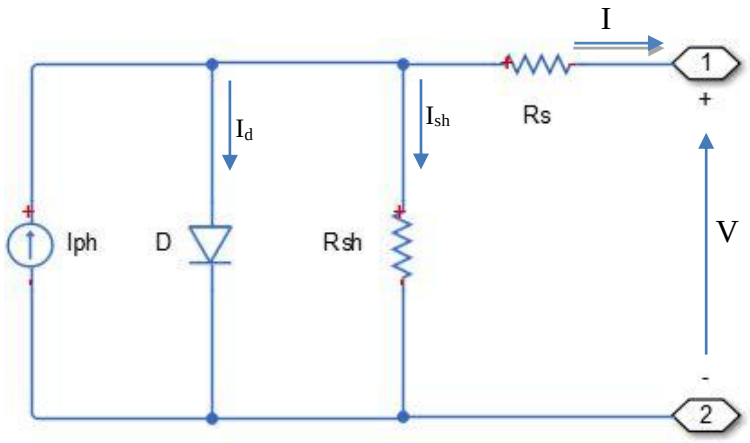

Figure 3-1 Solar cell single diode equivalent model

Where the equation that governs the current and voltage relationship as a function of the previously mentioned parameters is given by:

$$I = I_{ph} - I_0\left(\exp\left(\frac{V + I.R_s}{V_t}\right) - 1\right) - \left(\frac{V + I.R_s}{R_{sh}}\right)$$

Where I_{ph} ,R_{sh} ,R_s and I_0 are respectively the photocurrent, the shunt resistor, the series resistor, the diode saturation current, and V_t is the thermal voltage given by:

$$V_t = \frac{A.K.T}{q} \quad ;$$

and A,k,T and q are ideality factor, Boltzman constant, temperature and electron charge respectively [4].

Using the essential point of a PV cell characteristics curve, which are at the short-circuit where: $I=I_{sc}$ and V=0, and at the open-circuit with $V=V_{oc}$ and I=0, also at the maximum power point having $I=I_{mpp}$ and $V=V_{mpp}$, the unknown parameters R_{sh}, R_s and the ideality factor A can be determined by solving a set of equations with the help of numerical methods. Now, they are replaced in I-V equation to determine I_{ph} and I_0, and hence the five parameters are obtained, and can now be used in to build an accurate PV module model consisting of several cells in series with the help of Simulink.

3.3 PV array performance model

The Simulink tool in the MATLAB software has been used to model the photovoltaic array, where a Simulink block called the PV array is chosen, and used as PV module, where the number of cells in series is chosen 'N_s' as well as the number of strings inside the module 'N_p'. The cell's parameters are either provided by Simulink for predetermined modules, or defined by the user. The parameters defined for this block, are the open-circuit voltage, the short-circuit current, the voltage and current temperature coefficients and the maximum power point voltage and current coordinates. This block is pre-provided with a calculation algorithm to extract the cell's parameters based on a single diode model which are [I_{ph}, R_s, R_{sh}, I_0 and ideality factor A] depending on the entered values, which correspond to real PV modules, and are obtained from the datasheet provided by the manufacturer.

For this work, PV modules consisting of 60 cells attached in series, of which the datasheet to a real model is in appendix B. The main purpose of attaching several modules in series is to build up more voltage at the output of each panel, considering that the PN junction in each PV cell produces no more than 0.6V in most cases under normal operation. Now that every module have a maximum voltage of 39.8V, the current in this series is the same, it could have a maximum of 9.2A if we consider CT290MXX-02, the nominal maximum power of this module is about 290'Wp (V_{mpp}=32V, I_{mpp}=9.1A) at the STC.

The next step is to choose the dimension of the array, taking into consideration the voltage and the current desired at its output, which is also dependent on the adaptation blocks. Modules in series adds up the voltage to form a 'string'. Parallel strings allows the current's buildup. The array is chosen to have 6 modules in each string, and to have 4 strings. The nominal power for such array would be "6.96 W_{peak}" at STC. Bypass diodes have been connected to each module in order to protect it in case of partial shading or if there is reversed polarity.

The PV array built in Simulink is shown in appendix A, with N_s=6 and N_p=4.

3.4 The DC-DC converter

For this system modeling, the type of DC chopper that has been chosen is a buck converter which has the schematic shown in figure 4.2, the switching device used is an ideal switch characterized by a high frequency switching capacity. Controlled by the PWM generator, that generates a duty cycle which is corresponded to its input signal.

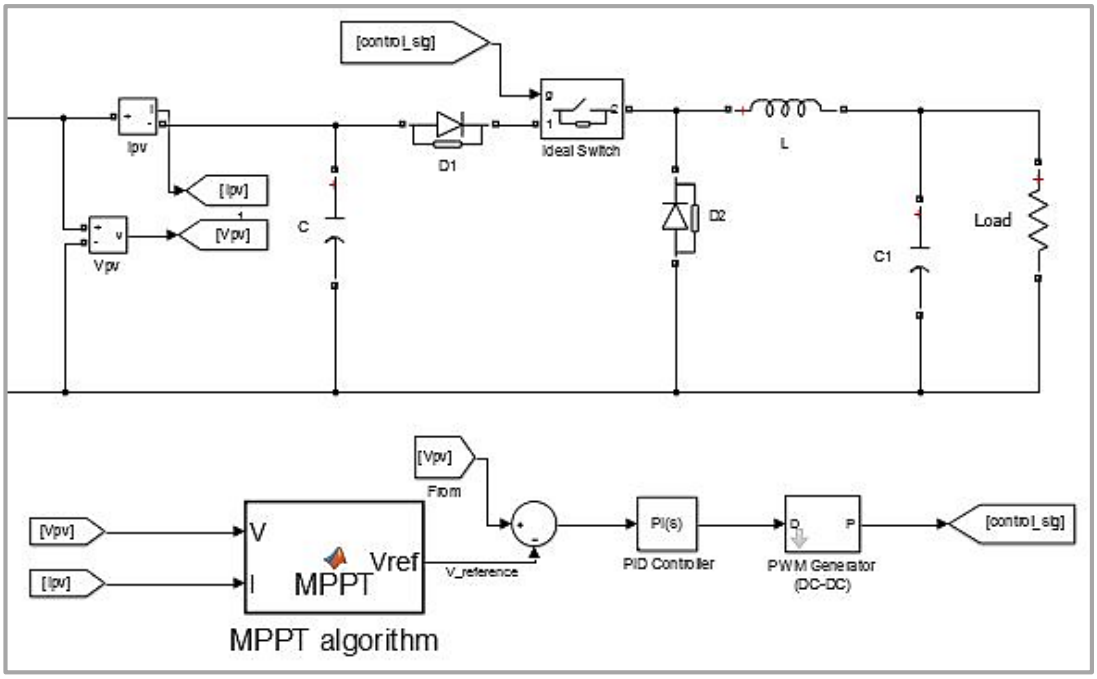

Figure 3-2 Buck converter.

The latter is generated by a PID controller, the compensation is made as to the difference between the actual PV output and the control voltage determined by the MPPT algorithm.

3.4.1 MPPT algorithm

As mentioned in the first chapter, the output power of the PV array has a maximum point that correspond to particular values of voltage V_{mpp} and current I_{mpp} which are unique and determined in case of fault-free operation of the system. The MPP tracking algorithm implemented is set to calculate a voltage "V_c" which is used as a reference voltage for the PID controller. This compensation, by changing the duty cycle on the switch control gate, drives the PV output voltage towards the reference, until the latter is determined and fixed by the algorithm which means the MPP is found, with a tolerance of 0.5% of the V_{MPP}.

- **The P&O algorithm:**

For applying this essential task of the system, the chosen algorithm is called "perturb and observe", which is characterized by its simplicity, quick response and less computational capacities requirements [23].

As the name suggests, the perturbation is made to the voltage level, where the step taken could be either positive or negative, and the according power change is observed. This principle is better explained using the flowchart in the figure 4.3. The step size chosen determines the accuracy of the algorithm in finding the MPP, the smaller the

step, the more accurate the result, however that is a trade-off with the computational efforts needed, and the response time in case of conditions change.

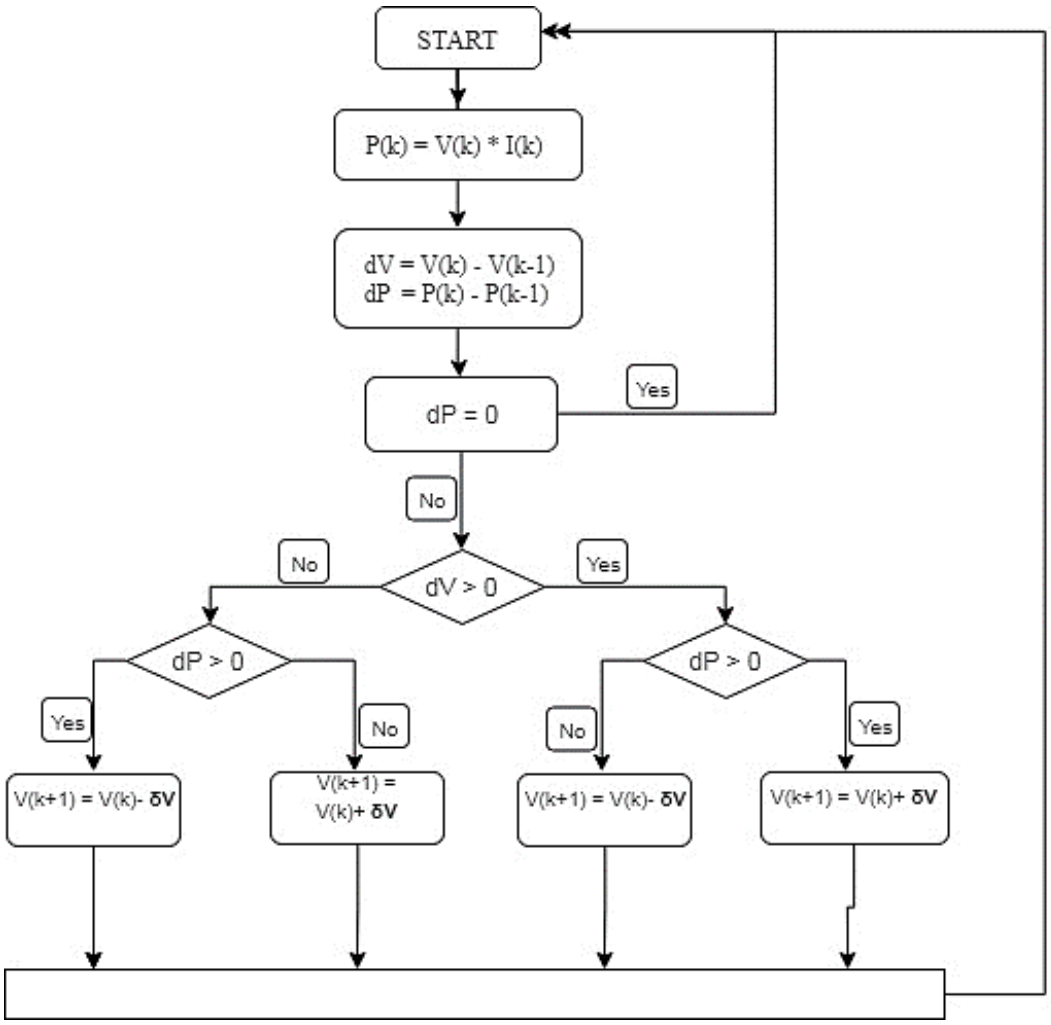

Figure 3-3 P&O - MPPT algorithm flowchart [24].

3.5 Quantifying system's performance parameters

Established by the International Energy Agency (IEA) Photovoltaic power System Program, the following parameters, the array yield (Ya), the reference yield (Yr), the final yield (Y_f) and the performance ratio (PR), are used to describe the overall system performance with respect to the energy production, solar resource and overall effect of system losses.[14]

These parameters are described in detail:

- **Reference yield (Yr)**

The reference yield (Yr) is the total in-plane irradiance (H) divided by the PV's reference irradiance (G_{ref}). It represents the equivalent amount of hours necessary for the

array to receive the reference irradiance. It is a function of the location, orientation of the PV array and weather variability. It is calculated using the equation:

$$Y_r = \frac{H}{G_{ref}} \text{ (Hours)}$$

Where:* H is the total-in-plane irradiance (Wh/m^2).

* G_{ref} is the reference irradiance at STC (= 1000 W/m^2). [14]

- **Array Yield (Y_a)**

The array yield is the energy generated by the PV array (Wh) divided by the rated output power of the PV array (W_p). It gives the number of hours which takes the installed PV system in order to produces its rated output DC power. The value of the array yield (Y_a) is calculated in Equation:

$$Y_a = \frac{E_{dc}}{P_{ref,STC}} \text{ (Hours)}$$

Where:

E_{dc}= energy generated by the PV array (Wh).

P_{ref}= maximum power output of the PV array (W_p). [4]

- **Final Yield (Y_f)**

The final yield is the net AC energy output (E_{Ac}) divided by the rated DC power (P_{ref}) (at STC) of the installed PV array. It represents the number of hours that the PV array would need to operate at its rated power to provide the same energy. The value of the final yield (Y_f) is calculated as:

$$Y_f = \frac{E_{Ac}}{P_{ref,\ STC}} \text{ (Hours)}$$

Where: E_{Ac}, is the output PV system energy (Wh).

P_{ref}, is the System rated power (W_p). [14]

- **Performance Ratio (PR)**

The performance ratio is the final yield divided by the array yield. By normalizing with respect to irradiance, The (PR) quantify the overall effect of losses on the rated DC output due to inverter efficiency, wiring mismatch and other DC-AC power conversion losses, PV module temperature, incomplete use of irradiance by reflection from the module front surface, soiling or snow, and component failures. The value of the performance ratio (PR) is calculated by the equation:

$$\text{PR} = \frac{\mathrm{Y_f}}{\mathrm{Y_a}} \text{ (Dimensionless)}$$

The PR has an average value from 0.4 to 0.8, large decrease in PR indicates abnormal events with severe impact on the performance, whereas, small decreases could be identified as an anomaly presence for which the cause is not identified by this parameter. [14]

3.6 PV array faults modeling:

A PV array performance model has been showed in the case of fault-free operation. In order to study the system behavior under each fault, the Simulink model shown in Appendix A is edited so that several faults are created, initially one at a time then combinations of different faults. The simulation allows to see the effect of each fault and the changes propagation from the parameters to the output variables. After creating the proper simulation for each of the mentioned faults, a comparison with the normal performance is made for both a single and group of faulty modules. This comparison is interpreted graphically with the IV characteristics curves.

3.6.1 Short-circuit fault

Any part of the system is affected by this fault, whether it is at module's output, within the module or at its connection with another one. Also, on the other different connections, among strings, bypass diodes. The first mentioned case is modeled in the figure 4.4 showing a short-circuit on the diode parallel to the modules 1 and 2.

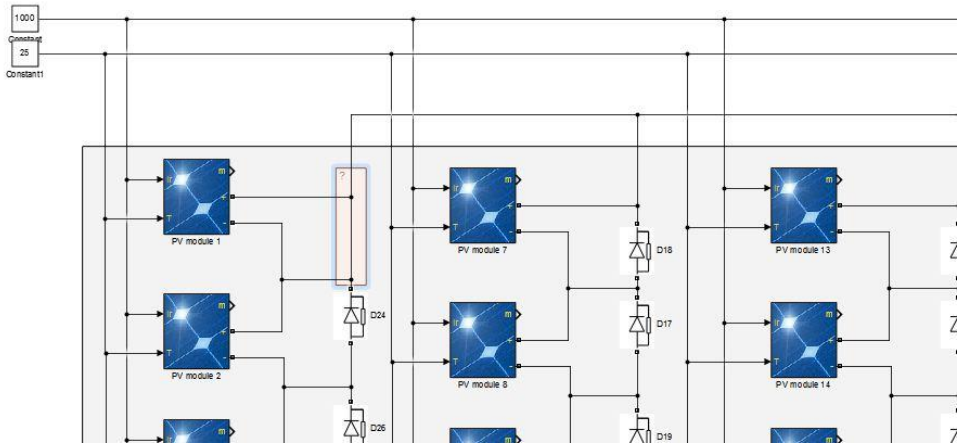

Figure 3-4 Short-circuit fault

After running this fault simulation, we have the figure, an IV curve of the normal performance is put to distinguish the change the short-circuit fault, when there is at first a single one, then with several modules short-circuited.

It is noticed that the open-circuit voltage drops in a directly proportional way with the number of modules short-circuited. The reduced value of voltage corresponds to: << V_{oc}/N_s>>, where 'V_{oc}' is the open-circuit voltage of each module (approximately 39.8V) and "Ns" is the number of modules in each string which in this case equals to 6. However the current remains unchanged with the occurrence of this fault. The array's IV curve is shown in the figure 4.5, for the normal operation, a single fault and 3 short-circuit faults.

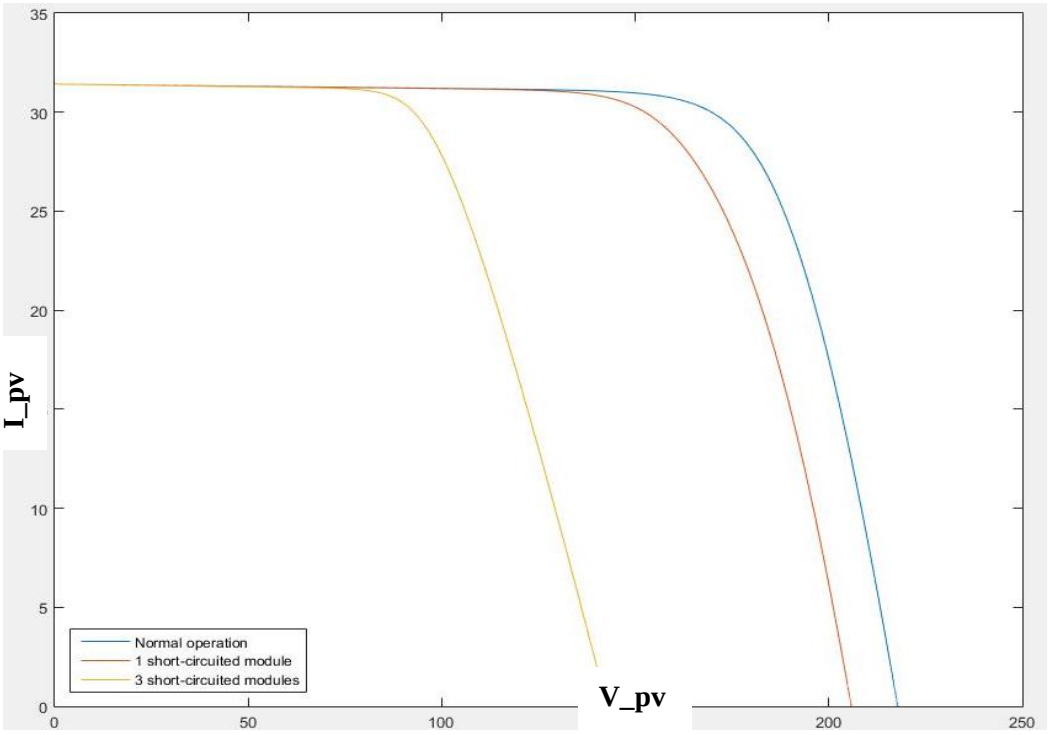

Figure 3-5 IV curves of normal and short-circuited modules

3.6.2 Open-circuit fault

The **Np** parallel strings connecting a number of modules in series could suffer this fault at any point, whether the reason is a completely defective module or a connection issue between two modules, or the blocking diode. This fault is modeled in the Simulink with the use of an ideal switch, that is in open position (has constant zero input). [4] Fig 4.6.

The result this fault has is noticed to be on the current level, since the strings adds up the current in the same node, and an open circuit means a zero current on the string, therefore the I_{sc} is reduced by a factor of 1/Np for each single fault. According to the chosen array dimension, we have four parallel strings, Np=4, therefore an open string

could reduce the current with 25% while the voltage is not affected. The figure 4.7 shows a normal, a single's and two faulty strings' I-V curves.

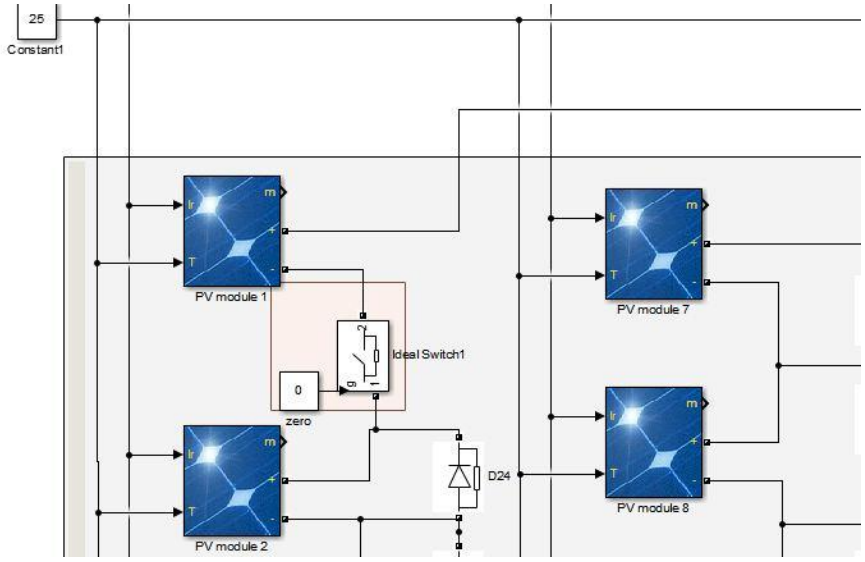

Figure 3-6 Open circuit fault

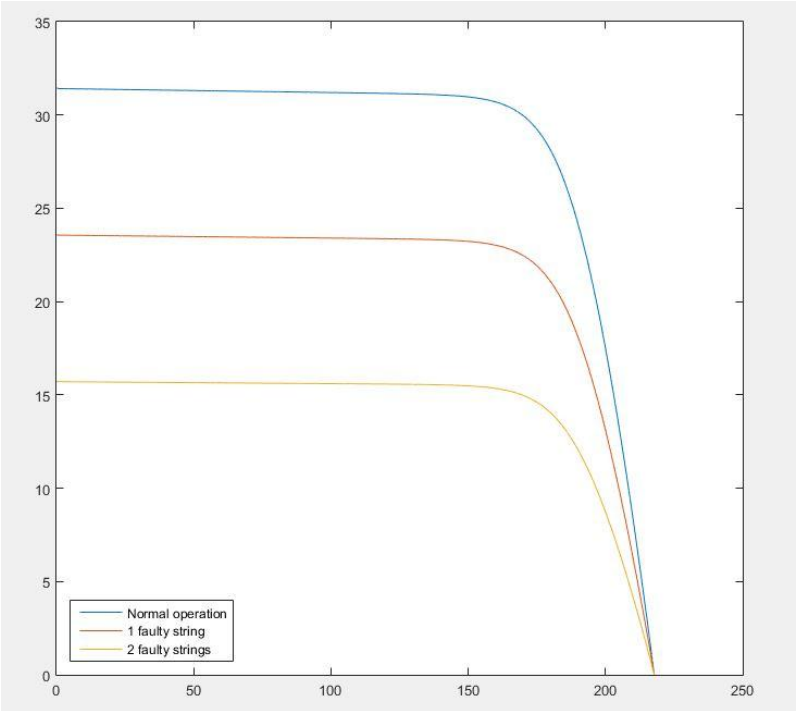

Figure 3-7 IV curve of normal and faulty strings

3.6.3 Partial shading

Due to the fact that partial shading is often faced in the PV installations, for either brief or long periods of time, and since it could cause significant power losses and change the output characteristics, it is considered a faulty state. It can be viewed as a non-uniformity of irradiance where significant difference is noticed, therefore, it is modeled

by supplying some of the modules to a different irradiance value as can be viewed in the figure 4.8. And, the effect ensued by this shading state, is observed in the figure 4.9, for two shaded modules.

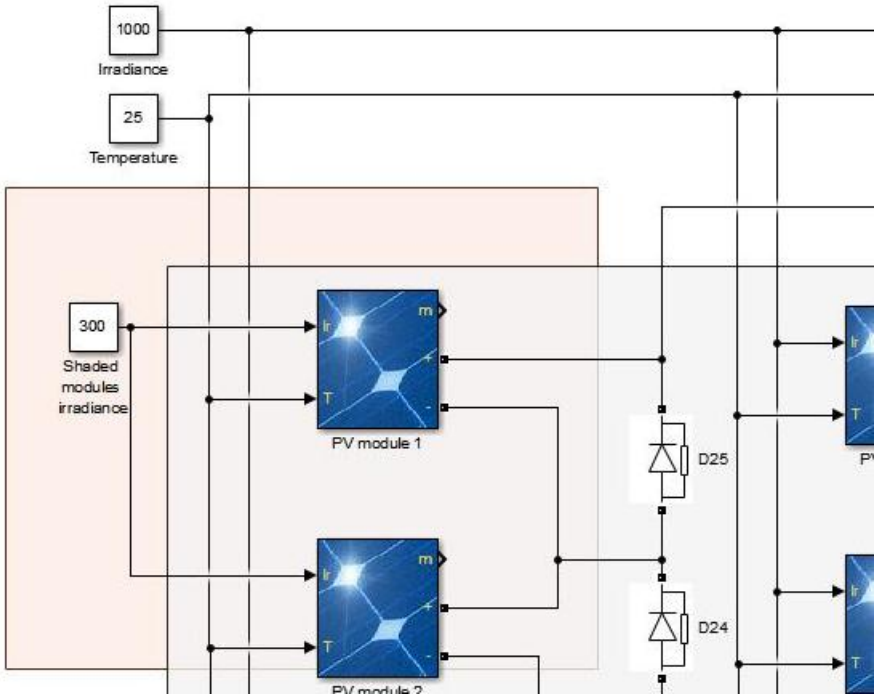

Figure 3-8 Two modules partially shaded

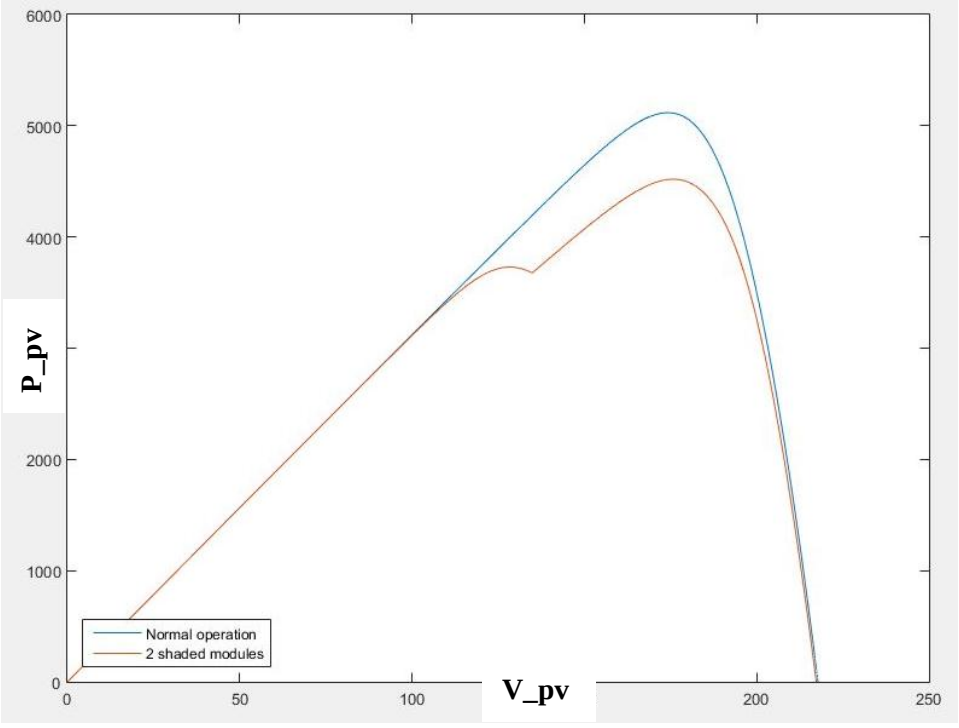

Figure 3-9 IV curve of normal and partially shaded sub-array

3.7 PV system's losses:

On both the DC and AC sides, the PV system endures losses, due to several causes. A quick overview of the main factors are displayed in the next figure:

- **Capture losses**

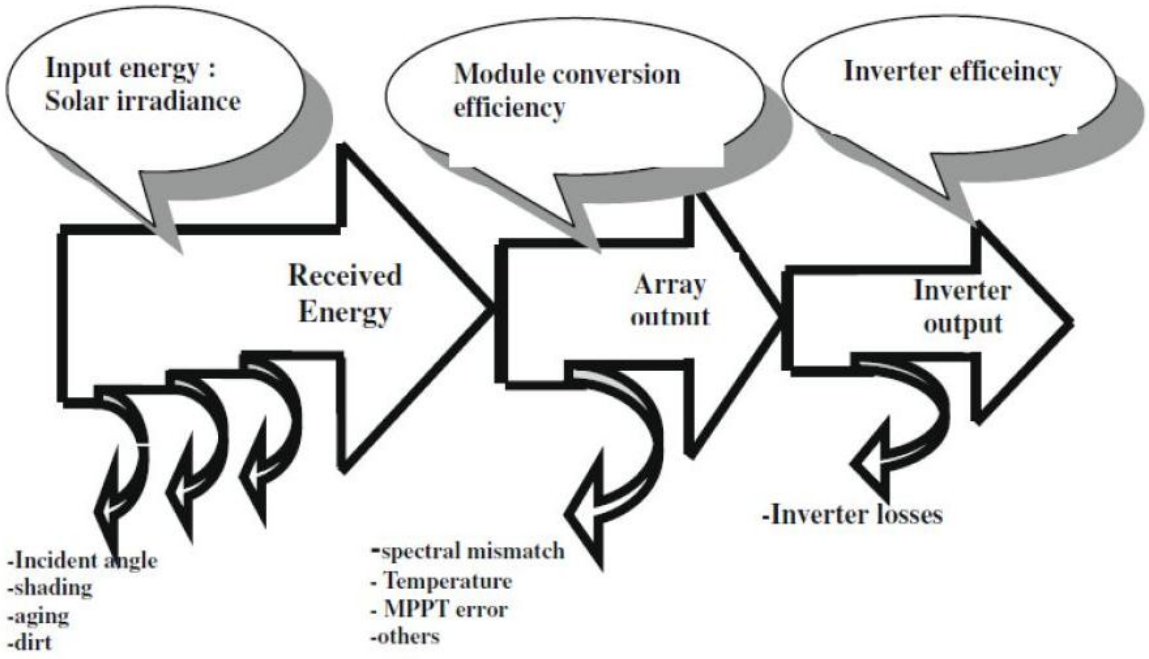

Figure 3-10 Loss mechanisms in PV systems.[3]

This kind of losses occur at the DC side of the PV system and they are attributed to operating temperature, PV efficiency temperature dependency, dependency on solar irradiance level, shading and losses when sunlight is at a high angle of incidence (AOI). The overall DC part losses are defined by the normalized total capture losses "L_c". By knowing performance parameters of the PV plant, one can calculate the capture losses by the following expression [15]:

$$L_c = Y_r(G,T) - Y_a(G,T) = \frac{H}{G_{ref}}(G,T) - \frac{E_{dc}}{P_{ref}}$$

where Yr(G, Tc) and Ya(G, Tc) are the reference and array yields, respectively, at real working irradiance, G, and real cell temperature T.

Furthermore, these global losses can be divided into two types of losses; thermal and miscellaneous capture losses denoted as (L_{ct}) and (L_{cm}), respectively [15].

- **Thermal capture losses (L_{ct})**

The actual temperature of the PV module differs from the nominal 25C° of the STC, therefore losses always exist and the system's efficiency does reduce. These thermal losses are due to the output voltage decrease when temperature rises beyond 25C°, as the

module has a negative temperature coefficient, (e.g. about "- 0.44/C°" for TSE100 at the maximum power point). The normalized thermal losses can be defined by the equation[15]:

$$L_{ct} = Y_a(G, 25°C) - Y_a(G, T)$$

- **Miscellaneous capture losses (L_{cm})**

In this class of losses we sum up all the other losses, such as wiring, dirt and snow accumulation, non-uniform irradiance, diodes and faulty operation if one of the components. The significant variation of this indicator may be interpreted as the existence of a fault. The miscellaneous capture losses are given by [4]:

$$L_{cm} = L_c - L_{ct}.$$

Fault detection system is based on continuous check of the measured miscellaneous capture losses. For this reason, we have established theoretical boundaries that the measured (L_{cm}) does not exceed. If these thresholds are surpassed the system is functioning in faulty state. These upper and lower boundaries are calculated by means of statistical approach and in case of PV system normal operation as represented by the expression:

$$L_{cm-sim} - 2\delta < L_{cm-meas} < L_{cm-sim} + 2\delta.$$

Where δ is the standard deviation [2].

3.8 Calculation of I_{sc} and V_{oc} of the Array:

Initially, we determine the I_{sc} and V_{oc} values for a single module.

- **Calculation of Isc_mod and Voc_mod of the (PV Module):**

For an arbitrary values of the irradiance and temperature, the short circuit current of a PV module, I_{sc_mod}, is given by the equation:

$$I_{sc_{mod}} = \frac{I_{sc\_mod\_r}}{1000}.G + \left(\frac{dI_{sc_{mod}}}{dT}\right)(T_{cell} - T_r)$$

Where $I_{sc\_mod\_r}$ and T_r are the short circuit current of the PV module and the temperature at for standard test conditions (STC: G = 1000 W/m2 and T = 25 °C) respectively, G is the actual irradiance on the PV module and T_{cell} is the real operating cell temperature.

And the open circuit voltage of the PV module, V_{oc_mod} is given by:

$$V_{oc\_mod} = V_{oc\_mod\_r} + \left(\frac{dV_{oc\_mod}}{dT}\right)(T_{cell} - T_r) + V_t.\ln\left(\frac{I_{sc\_mod}}{I_{sc\_mod\_r}}\right)$$

Where $V_{oc\_mod\_r}$ is the open circuit voltage of the PV module at STC and Vt is the thermal voltage. [4]

The temperature coefficients $\left(\frac{dI_{sc_{mod}}}{dT}\right)$ and $\left(\frac{dV_{oc\_mod}}{dT}\right)$ are given in the datasheet of the PV module. The current coefficient has a positive sign in contrast of the negative sign of the voltage coefficient.

In the work done by [4], after tracing the IV curves, the values of V_{oc_mod} and I_{sc_mod}, calculated by these equations are accurate, and can be reliable, they have an error of about 3%. Therefore, these variables don't need monitoring as they are calculated by the MATLAB software for any given values of irradiance and temperature.

- **The PV array :**

For a PV array that has $\mathbf{N_p}$ parallel string, with each one of them having $\mathbf{N_s}$ module connected in series, the open circuit voltage and the short circuit current are given by the following expressions:

$$I_{sc} = N_p * I_{sc_{mod}} = N_p.\left(\frac{I_{sc_{mod_r}}}{1000}.G + \left(\frac{dI_{sc_{mod}}}{dT}\right)(T_{cell} - T_r)\right)$$

$$V_{oc} = N_s * V_{oc_{mod}} = N_s.(V_{oc_{mod_r}} + \left(\frac{dV_{oc_{mod}}}{dT}\right)(T_{cell} - T_r) + V_t.\ln\left(\frac{I_{sc_{mod}}}{I_{sc_{mod_r}}}\right)).$$

3.9 Conclusion

In this chapter, a PV array model has been built using Simulink, in order to emulate the performance of real array with the defined configuration. Normal state is first modeled, after which, the faults considered for the diagnosis are modeled, in addition to their effect on current and voltage characteristics, and the power losses induced by these faults.

CHAPTER 4 : FAULT DETECTION AND DIAGNOSIS

4.1 Fault indicators

The previous procedure (L_{cm} threshold) indicates the existence of anomalies when the losses exceed the thresholds, however it does not determine the failure cause or type. Therefore two indicators are defined to point out the abnormal system's behavior by evaluating the deviation of the measured current and voltage values at the PV array output with the correspondent simulated values. These unitless indicators are given by:

$$Q_v = \frac{V_{pv\_sim}}{V_{pv\_meas}}$$

$$Q_c = \frac{I_{pv\_sim}}{I_{pv\_meas}}$$

Where IP_{V_meas} and V_{PV_meas} are the current and voltage measured at the output of the PV array respectively, and IP_{V_sim} and V_{PV_sim} the results obtained for those parameters in the simulation of the PV system behavior by using real irradiance and temperature [16]. Analysing the ratios, the probable malfunction is found following the flowchart in the figure 5.1:

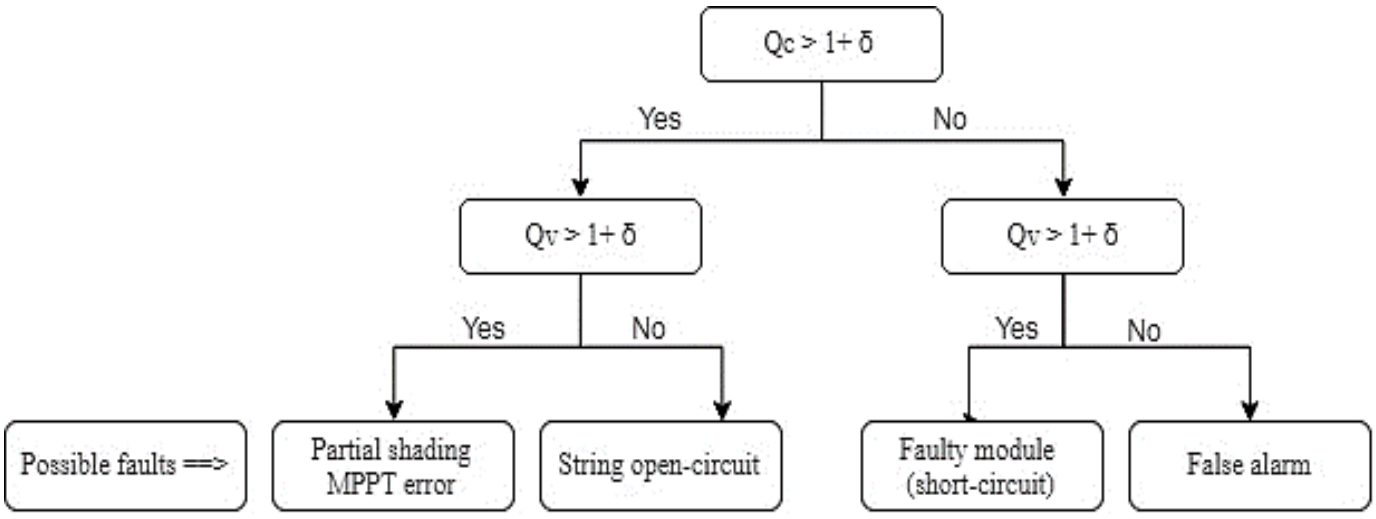

Where 'δ' is the value of the standard deviation of the difference between the actual and simulated values of the array, when it's operating fault-free.

4.1.1 Voltage and current indicators for fault detection:

The fault diagnosis system based on the energy yields is not as reliable as the current and voltage ratios mentioned previously, however the computational effort and

the requirement of simulation use, another method which is also based on the current and voltage values where the point we are taking into consideration is the maximum power point.

This method has been first developed in [16], for several types of PV modules with different series and parallel cell configuration.

The next current and the voltage indicators, are with respect to the short circuit current (I_{sc}) and the open circuit voltage (V_{oc}), respectively. The latters are functions of temperature and irradiance. These new indicators are given by the expressions:

$$U_v = \frac{V_m}{V_{oc}}$$

$$U_c = \frac{I_m}{I_{sc}}$$

where V_m and I_m are the voltage and current of the maximum power point (MPP) at the PV array DC output respectively, I_{sc} is the short circuit current of the PV array and V_{oc} the open circuit voltage of the PV array.[17]

Considering the fault-free operation of the system, two new variables are introduced, which characterize this state. They define the expected value in normal operation, they represent the value to which the indicators above are compared to determine the presence of a fault. They're given as:

$$U_{v\_r} = \frac{V_{m\_r}}{V_{oc}}$$

$$U_{c\_r} = \frac{I_{m\_r}}{I_{sc}}$$

where V_{m_r} and I_{m_r} are the voltage and current at the maximum power point (MPP) of the fault-free PV array DC output in the normal operation state, respectively.

Introducing these variable allows us to normalize the indicator's values, for better assessment of the threshold setting.

When the system suffers no fault the U_v and U_c measured should be as close as possible to U_{v_r} and U_c respectively [17].

4.2 System's evaluation under faults:

After calculating the indicators reference, $\mathbf{U_{v\_r}}$ and $\mathbf{U_{c\_r}}$, the threshold is dependent on the configuration of the PV array, namely, the number of the parallel (**Np)** and the series (**Ns)** modules in the array.

As discussed in the second chapter, the current is affected by the open circuit fault, hence the indicator $\mathbf{U_c}$ would drop below the reference value and the threshold. On the other hand, the voltage indicator $\mathbf{U_v}$ goes below the set threshold in case of short-circuit faults.

4.2.1 Open-circuit fault:

While the array has N_p parallel strings the overall current of the PV array is given by: << $\mathbf{I_m = N_p * I_{m\_mod}}$ >> where I_{m_mod} is one module's current. Therefore, the fault-free indicator (U_{c_r}) can be written as:

$$U_{c\_r} = N_p \frac{I_{m\_mod}}{Isc}.$$

Now, the presence of one single open circuit would be interpreted by the equation of the faulty string current indicator:

$$U_{c\_f} = \frac{(N_p - 1).I_{m\_mod}}{Isc} = \frac{N_p.I_{m\_mod}}{I_{sc}} - \frac{I_{m_{mod}}}{I_{sc}} = U_{c\_r} - \frac{U_{c_r}}{N_p} = U_{c\_r} - f_o$$

Where: $f_o = \frac{U_{c\_r}}{N_p}$ is the value by which a single open-circuit fault can reduce the current indicator value.

For $\boldsymbol{U_{c\_f}}$ being the faulty string current indicator for at least one fault, it is set to be the threshold below which the existence of a fault is detected [17]. In order to reduce the possibility of false alarms a tolerance "**ε**" is introduced to lower the threshold value, the tolerance value is chosen to vary from 0.002 to 0.02. Thus the threshold is set to be:

$$TU_{c\_f} = (U_{c\_r} - f_o) * (1 - \varepsilon)$$

Setting this threshold allows to detect the open circuit fault's occurrence, however, to reckon how many strings are faulty (open), we need other determined values of the indicator U_c that could reflects the number of faults existing. These points are defined by the equation:

$$T_{cn} = (U_{c\_r} - n.f_o) * (1 - \varepsilon)$$

Where 'n' is the number of the faulty strings in the PV array, which varies from 0 to N_p [3]. Now, the number of the faulty strings is determined by the location of the $\underline{U_c}$ value with respect to these new multiple values determined. An case example is when the occurrence of two faults which corresponds to surpassing the value:

"$T_{c2} = (U_{c\_r} - 2.f_o) * (1 - \varepsilon)$", however not reaching the established value

"$T_{c3} = (U_{c\_r} - 3.f_o) * (1 - \varepsilon)$", i.e. the expression $T_{c2} > U_c > T_{c3}$ means that two strings are faulty.[3]

4.2.2 Short-circuit fault

Considering the normal operation, the DC voltage output of the array is aggregation of the series modules voltages per string, that means, the reference voltage indicator can expressed as: $U_{v\_r} = N_s \frac{V_{m\_mod}}{V_{oc}}$.

The short-circuit happening reduce the string voltage by a V_{m_mod} value. The expression for one short-circuited module is given as:

$$U_{v\_f} = \frac{(N_s - 1).V_{m\_mod}}{V_{oc}} = \frac{N_s.V_{m\_mod}}{V_{oc}} - \frac{V_{m\_mod}}{V_{oc}} = U_{v\_r} - \frac{U_{v_r}}{N_s} = U_{v\_r} - f_s$$

Where "$f_s = \frac{U_{v\_r}}{N_s}$" is the value of difference between a normal operation indicator U_{v_r} and a single faulty module.

Since U_{v_f} is the voltage value that points the occurrence of one short-circuit fault, the threshold is then set at it and following the same procedure as with the open-circuit fault, the tolerance "**ε**" is again introduced to avoid false alarms. Thus, the threshold value is U_{v_f} corresponding one short-circuited module, and given by:

$$TU_{v\_f} = (U_{v\_r} - f_o) * (1 - \varepsilon)$$

Having a fault threshold set-up, one more point needs evaluation, which is the number of short-circuit faults occurring, based on the same principle used with the open-circuit fault, the new indicators based on the U_{v_f} are calculated by the expression:

$$T_{vn} = (U_{v\_r} - n.f_o) * (1 - \varepsilon)$$

Where 'n' is the number of the short-circuited modules, which varies from 0 to the number of modules per string $\mathbf{N_s}$. The value of U_v given when an "n<Ns" short circuit fault occurs, is bound as shown in the expression:

$$T_{vn} > U_v > T_{c\_n+1}.$$

4.2.3 Partial shading

When some of the PV modules are shaded, the voltage and current levels are decreased significantly, and for protecting the modules, the bypass diode is activated whenever that happens. However, the result of this fault creates more than one power peak and inflection points at the IV characteristics curve.

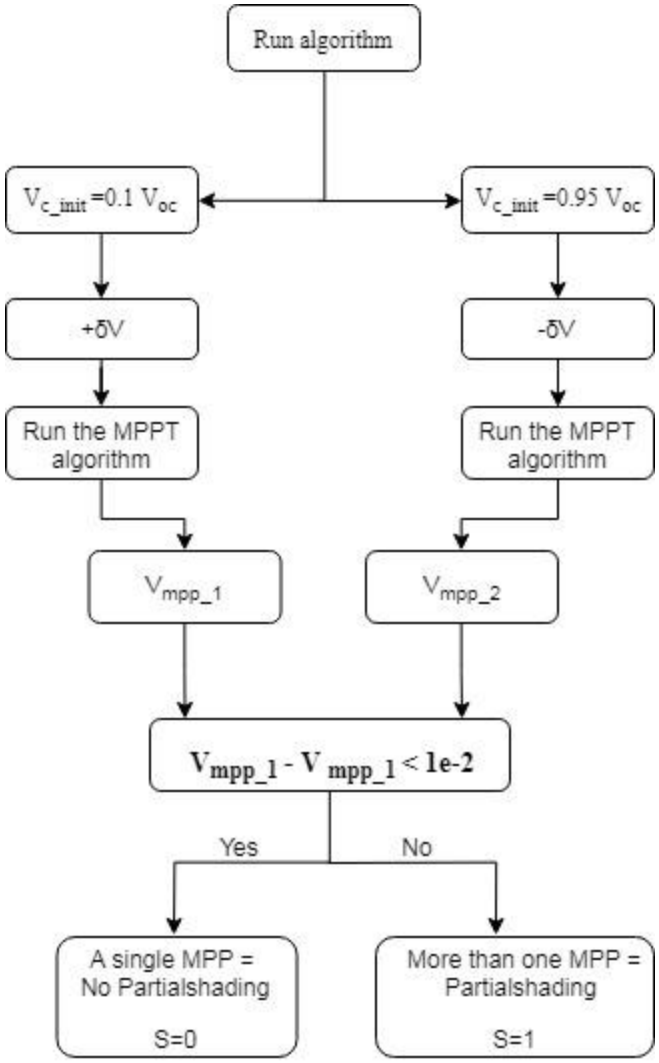

Figure 4-2 Partial shading detection algorithm flowchart

In this diagnosis system, in order to detect the existence of partial shading, we determine if the power curve of the PV array has more than one local maximum, for that purpose, an algorithm is set to calculate power variation as function of the current and voltage, where the latter's variation is the one being controlled. Since we suspect the existence of at least two local maximums, the tracking algorithm is run twice from two different directions. The first starting from V_c=0.1 V_{oc}, with a positive variation '+δV' until a maximum point is found. Whereas the second starts from V_c= 0.95 V_{oc}, and keeps decreasing with '-δV' till a local maximum is reached. The condition set to detect the existence of partial shading, is that the V_{mpp1} and V_{mpp2} have different values, otherwise we have the same MPP and the array is not under a partial shading condition.

This operation is better shown in the flowchart in the figure 5.2.

For multiple dissimilarities in levels of irradiance onto the PV array, the expected array characteristics change is more severe, and the power will have more power peak points resulting more losses and efficiency drop, also increasing the possibility of MPP tracking error. The IV and PV curves of the array having different levels of irradiances are in the figure 5.3.

The described behavior above is noted on the figure 5.3 generated by the

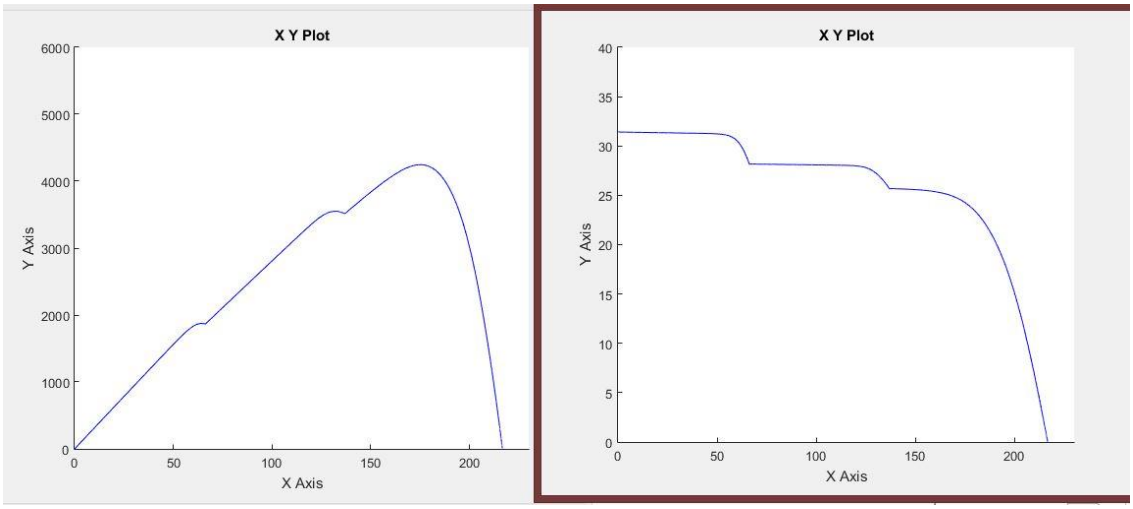

Figure 4-3 PV and IV curves of array under partial shading state

simulated array for 3 different irradiance levels, 2 modules under 600(w/m²) irradiance, and 2 modules shed by 300 (w/m²) while the rest of the PV array is in not shaded, their irradiance is 900(w/m²).

4.3 Diagnosis system validation

After choosing the PV array configuration and the diagnosis method, the ability of the system to detect the occurrence of a single or multiple faults at the same time is of the essence. Moreover it is supposed to identify these faults correctly and spot the overlapping faults.

For that goal, a few test cases have been chosen, where multiple and different faults occurred simultaneously, and the diagnosis algorithm's response has been noted. The table 5.1 contains the test faults created in the PV system.

Table 4-1 Selected faults for diagnosis system validation

Cases	Faults
F1	Two short-circuited module
F2	four short-circuited modules
F3	One faulty string
F4	Two faulty strings
F5	Four partially shaded module
F6	Eight partially shaded modules
F7	The simultaneous occurrence of faults F1 and F4
F8	The simultaneous occurrence of faults F2 and F3
F9	The simultaneous occurrence of faults F1 and F5
F10	The simultaneous occurrence of faults F3 and F6

The diagnosis system is based on the comparison of the current measurements with the ones known to be healthy. Hence, the main system's data in the healthy case, is given in the next table, where the first three variables are given for STC conditions, however the indicators Uc and Uv describe the system under all healthy states. These measurement are taken as the average of numerous simulations effectuated, and they're characterized with a standard deviation of (< 1.5 %) of the variables' means.

Variable	Normal value
I_{mpp}(A)	29.3
V_{mpp}(V)	174
P_{mpp} (W)	5100
U_{c_ref}	0.93
U_{v_ref}	0.80

Table 4-2 Normal variables' values

The first short circuit fault occurred at time t=0.5s, this fault perturbs the operating point of the dynamic system and after a transient period, the system determines the new MPP and therefore the current and voltage change (U_c and U_v correspondingly), and the fault is identified as shown in the figure at time t=0.53s, where the variable 'sh' is the number of short-circuit faults occurring, which is currently '1'. Another similar faults are created in the same string at time t_1 = 1s and t_2 =1.5s, which we notice as the indicator

drops to zero for a transient period of 0.03s, and then determines the existence of the faults which is 2 and 3 respectively. The response described is shown in **figure 4.4**.

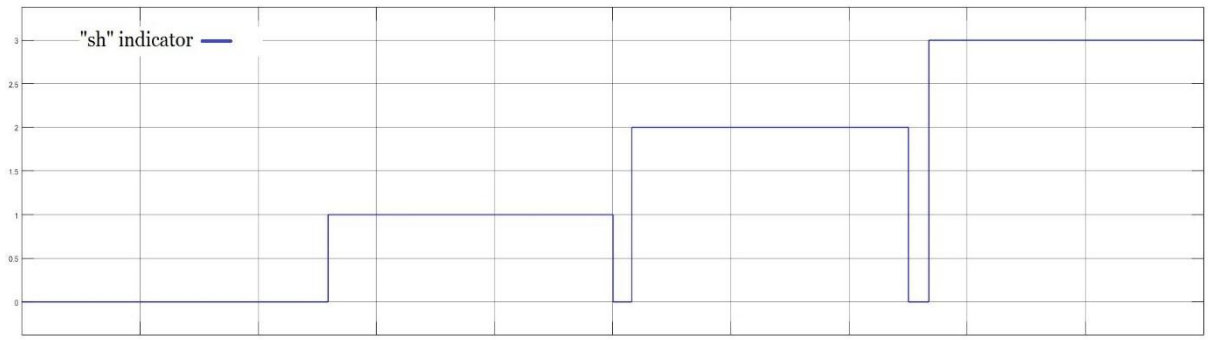

Figure 4-4 Sh indicator when testing 3 short-circuits

As expected, the current level is not affected by this fault, as for the voltage, it is noticed that it drops to (158V - 128 V - 93 V) at the MPP recalculated after the occurrence of each fault, instead of the nominal value. Correspondingly, the values of the indicator U_v change to 0.72, 0.59 and 0.42 respectively. The variations are shown in **figure 4.5**, for V_{pv} as for $U_{\underline{v}}$.

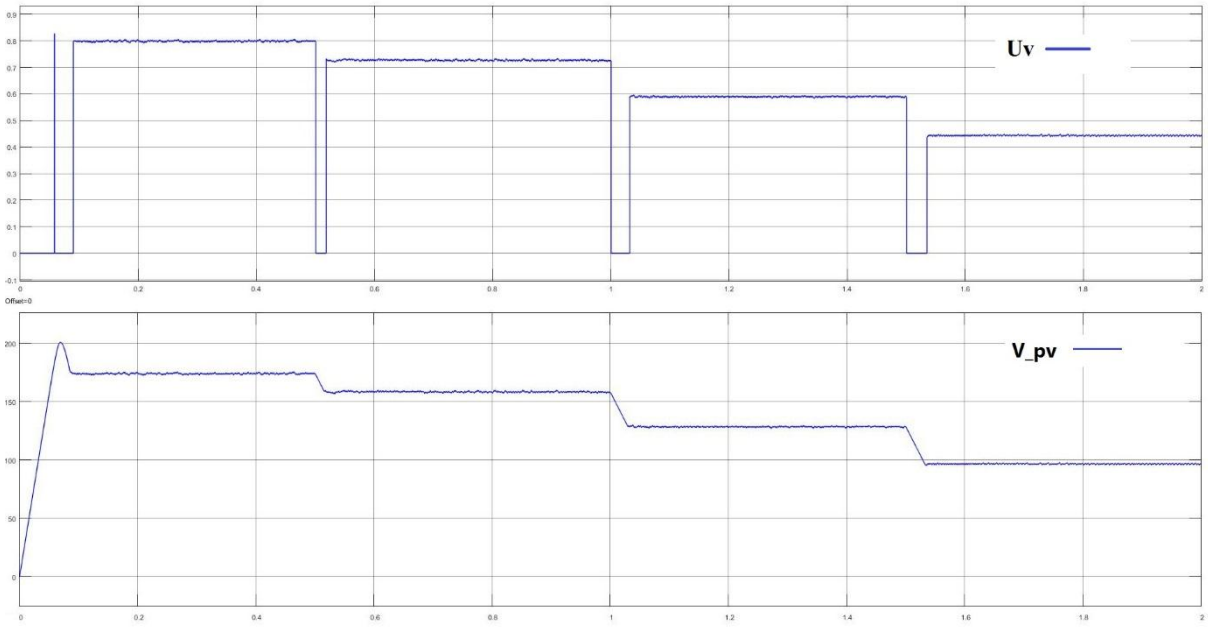

Figure 4-5 Voltage indicator and array voltage with multiple faults occurrence

Since the voltage is the variable affected by such fault, the current indicator is not changed, and does not leave the 1.5% margin of error. And so is the case for I_m except at the transient periods.

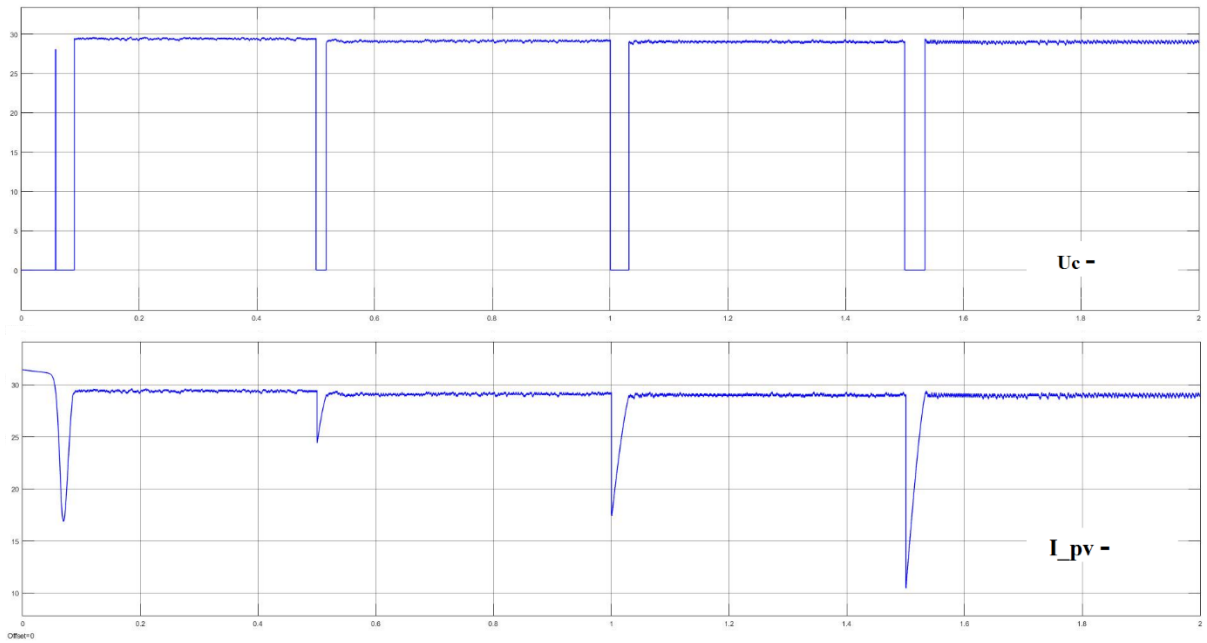

Figure 4-6Current indicator and array current with multiple faults

The second case is made for faults three and four, now, the current indicator is the one having a drop. At time t= 0.09 s, the first fault is created, and after a transient time, at time t= 0.095 s, the new U_c is measured and the alarm for the open-circuit fault is high with a value of '1'. Furthermore, the same fault is recreated for another string and at t= 0.11 s, the number of fault changes to "2" as interpreted by the variable "op" in the figure.

It is noticed that the faulty string produce a significant power loss, yet the MPP is barely perturbed with respect to the maximum power point voltage (Vmpp).

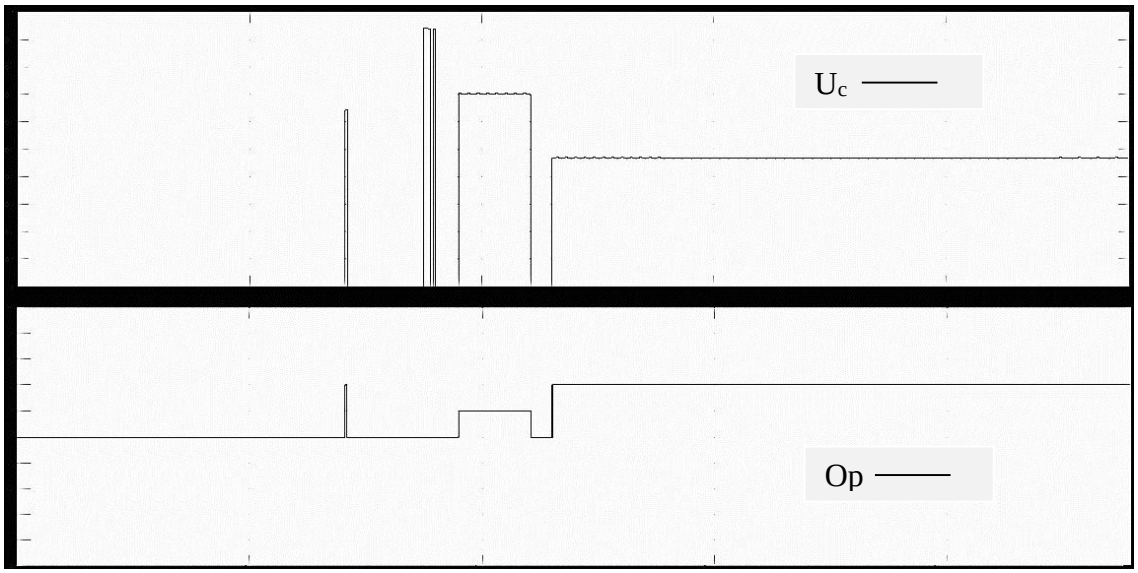

Figure 4-7 Value of current indicator and open circuit variable

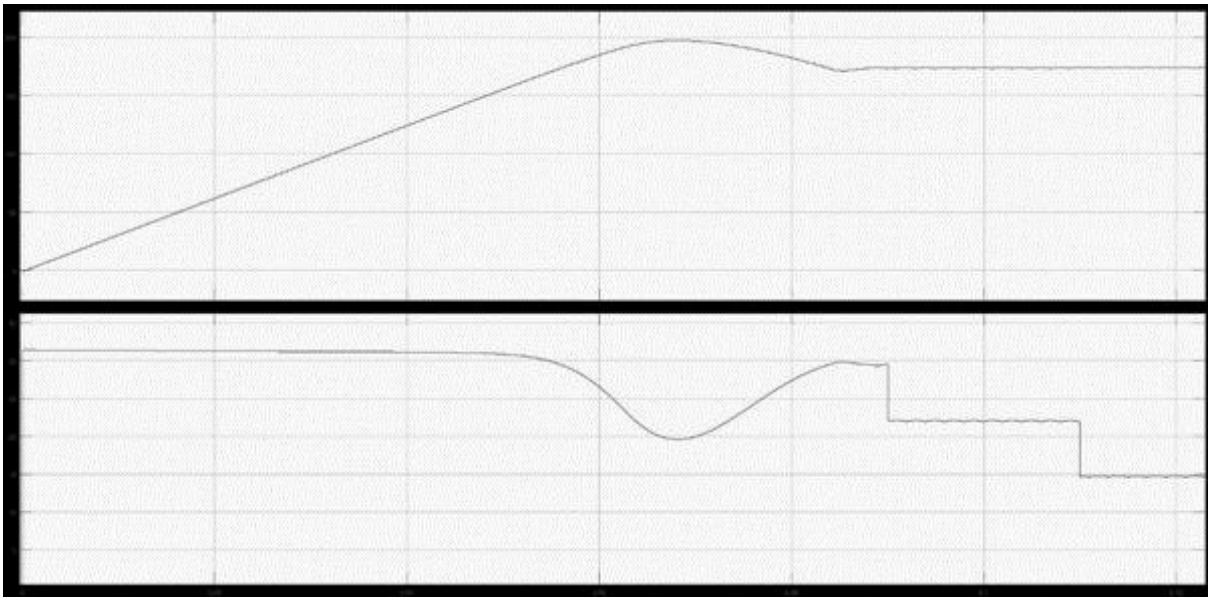

Figure 4-8 Voltage and current of th array

The next case is made for partially shaded modules of the array, having an irradiance of 500(W/m²), which is half the value delivered to the rest of the modules. As discussed before, a new local maximum point is created dissimilar to the actual MPP, and the algorithm aims to determine the voltage at which this maximum is formed. Having different values Vmpp sets the shading indicator to 1. As for keeping the system in operation in this case, the maximum power point is the one chosen after a comparison between, P_{mpp1} and $P_{mpp2.}$

The algorithm part determining the existence of the partial shading is independent from the other faults evaluating algorithm, and it is also effectuated previous to them.

Starting from $t=0_{(s),}$ the system takes time t= 0.045s to determine the Mpp1, and afterwards starting the next iteration till t= 0.105s at which Mpp2 is determined, then the comparison is made. Then the system interfaces the shading indicator value of '1' or '0', corresponding to the existence and non-existence of shading.

In the **figure 4.9** the I_{mpp} and V_{mpp} are shown as the algorithm runs, and the zero value corresponds to the system being in state of calculating the MPP.

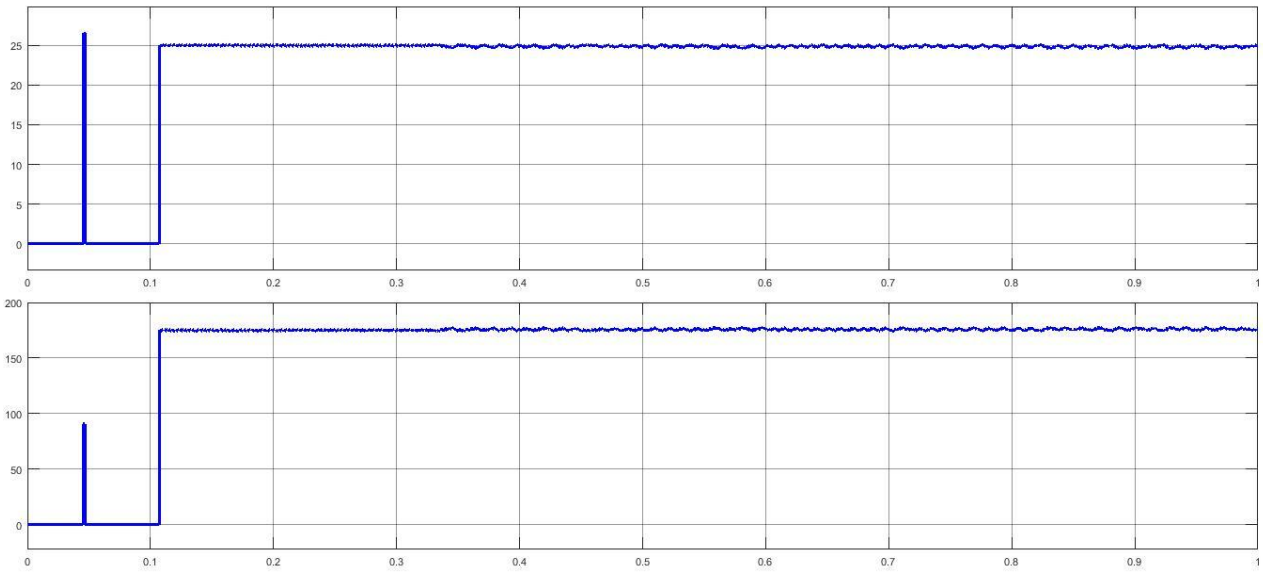

Figure 4-9 Peak I and V of the PV array under partial shading

We can notice that the first peak values are dissimilar to the second's, which means the existence of partially shaded modules. At M_{PP2} the system generates higher power, therefore it is chosen as the operating point.

In order to avoid wrong indications, the partial value indicator is set to determine the state only at t = 0.27 s, which is shown in the next figure since we have a partial shading.

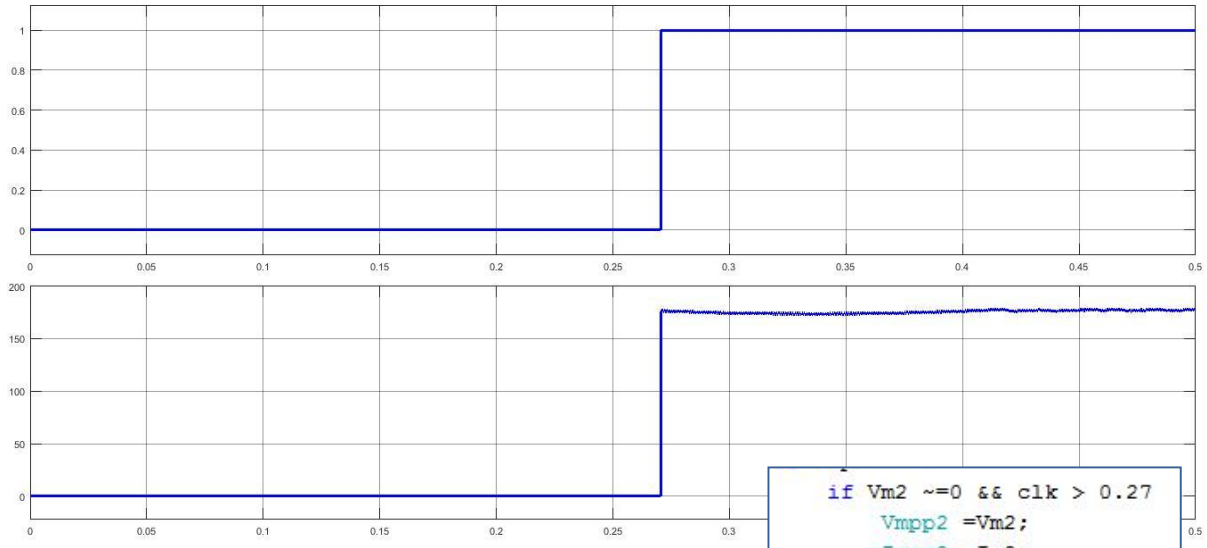

```
if Vm2 ~=0 && clk > 0.27
    Vmpp2 =Vm2;
    Impp2 =Im2;
    secc= 1;
end
```

Figure 4-10 The shading indicator

Another condition is made for the system, which is in case of irradiance changes, this variation alters all the local maxima, thus as the MPP is tracked continuously, the algorithm is re-run to check whether the partial shading is still existent.

Conclusion

After implementing the detection algorithm in MATLAB for the three types of faults above, the occurrence of these faults is accurately detected and interpreted. Despite successfully identifying the type of fault as well as their number, this method adopted lacks the ability to isolate the faults and locate the defective component. This latter requires more work based on the artificial intelligence methods to compensate for the lack of redundant data from within the system.

CONCLUSION

In this work, a fault diagnosis procedure has been conducted for the PV array. After going over the PV system components and characteristics, and choosing the configuration of the array under study, available methods of fault detection are stated. After which, the indicators have been chosen to monitor the possible occurrence of three types of faults which are the short-circuit, the open-circuit and the partial shading. Where the latter has a wider variation of possible states which are all faulty with dissimilarities in their effect, and hence the algorithm used in unlike the formers. For the purpose of increasing efficiency and reducing the possible damage for the system components due to faults propagation, the diagnosis process is required for all the PV systems.

For future works, other fault detection methods may be considered in light of widening the range of the faults identified within the system. Moreover, as the solar energy industry is growing, the fault detection in grid-connected PV system will be considered.

Bibliography

[1] https://en.wikipedia.org/wiki/Photovoltaic effect.

[2] L.Douibi Lahcene - Zegtouf Dhia Eddine "Automatic Monitoring and Fault Detection of Grid Connected Photovoltaic Systems", IGEE, 2013.

[3] M. Da Silva- "Analysis of new indicators for Fault detection in grid connected PV systems for BIPV applications" , UNIVERSIDADE DE LISBOA, 2014.

[4] Wafiya CHINE *« Contribution au diagnostic des défauts dans les systèmes photovoltaïques »,* Université MED Seddik BEN YAHIA – Jijel

[5] A.Chaudhary S.Gupta, D.Pande, F.Mahfooz, G.Varshney - effect of Partial Shading on Characteristics of PV panel using Simscape – October 2015. Int. Journal of Engineering Research and Applications

[6] Fault-Diagnosis Applications Model-Based Condition Monitoring: Actuators,

Drives, Machinery, Plants, Sensors, and Fault-tolerant Systems.

[7] McEvoy, A., Markvart, T. And Castañer, L., 2012. Pracical Handbook of Photovoltaics Fundamentals and Applications.

[8] Y. Yagi, H. K., 2003. Diagnostic technology and an expert system for photovoltaic systems using the learning method. Solar Energy Material & Solar Cells, 655-663.

[9] L.Bun, Détection et localisation de défauts pour un système PV, Thèse de doctorat, université de Grenoble, 2011.

[10] Emmanuel Kymakis - Performance analysis of a grid connected Photovoltaic Park on the island of Crete, (2009). Article in Energy Conversion and Management.

[11] Lobrano V., Orioli A., Cuilla G., Di Gangi A., An improved five-parameter model for photovoltaic modules,2010. Article In Solar Energy Materials & Solar Cells.

[12] http://mathworks.com/help/physmod/elec/ref/solarcell.html

[13] http://www.elecssol.com/

[14] Cristian P. Chioncel, 2.Dieter Kohake, 3.Ladislau Augustinov, 4.Petru Chioncel, 5 .Gelu Ovidiu Tirian. Yield Factors Of A Photovoltaic Plant. 2010. Acta Technica Corviniensis – Bulletin Of Engineering.

[15] S.Silvestre, A.Chouder, E.Karatepe – 'Automatic fault detection in grid connected PV systems', 2013. Solar Energy 94.

[16] S.Silvestre, M.Silva, A.Chouder, D.Guasch, E.Karatepe - New procedure for fault detection in grid connected PV systems based on the evaluation of current and voltage indicators, 2014. Energy Conversion and Management.

[17] S.Silvestre, S.Kichou, A.Chouder, G.Nofuentes, E.Karatepe "Analysis of current and voltage indicators in grid connected PV (photovoltaic) systems working in faulty and partial shading conditions, 2015. The Energy journal.

[18] Ishaque K., Salam Z., and Taheri H., Simple, fast and accurate two-diode model for photovoltaic module, Article *in* Solar Energy Materials and Solar Cells 95(2):586-594, 2011.

[19] https://www.civicsolar.com/support/installer/questions/what-blocking-diode.

[20] Z. Jaffery, A.K. Dubey, Irshad, A.Haque, "Scheme for predictive fault diagnosis in photo-voltaic modules using thermal imaging", *in* Infrared Physics & Technology 83, 2017.

[21] Miwa M., Yamanaka S., Kawamura H. and Ohno H., Diagnosis of a Power Output Lowering of PV Array with a (-dI/dV)-V Characteristic , presented at the Photovoltaic Energy Conversion, Conference Record of the 2006 IEEE 4th World Conference on Waikoloa, HI.

[22] CertainTeed Solar US SERIES 60 CELL solar modules - CT290MXX-02 datasheet.

[23] A.Atallah, Almoataz, Y. Abdelaziz, R.S. Jumaa, Implementation Of Perturb And Observe Mppt Of Pv System With Direct Control Method Using Buck And Buck-boost Converters, Emerging Trends in Electrical, Electronics & Instrumentation Engineering: An international Journal (EEIEJ), Vol. 1, No. 1, February 2014 ,Egypt.

[24] G.Badii Hemidet A., O.HASNAOUI, R.Dhifaoui, Experimental Study of MPPT Algorithms for PV Solar Water Pumping Applications, 2014 conference paper, Conference: IREC 2014, At Hammamet - Tunisia.

[25]L. Doukovska, S. Vassileva, Ai-Based Diagnostics for Fault Detection And Isolation In Process Equipment Service, Institute of System Engineering and Robotics - Bulgarian Academy of Sciences, 2010.

[26] T.Bouthiba, Artificial Neural Network-Based Fault Location in Ehv Transmission Lines.

[27]M.Louzazni, E.Aroudam, An intelligent Fault Diagnosis Method Based on Neural Networks for Photovoltaic System, 2014. International Journal of Mechatronics, Electrical and Computer Technology.

APPENDICES

Appendix A

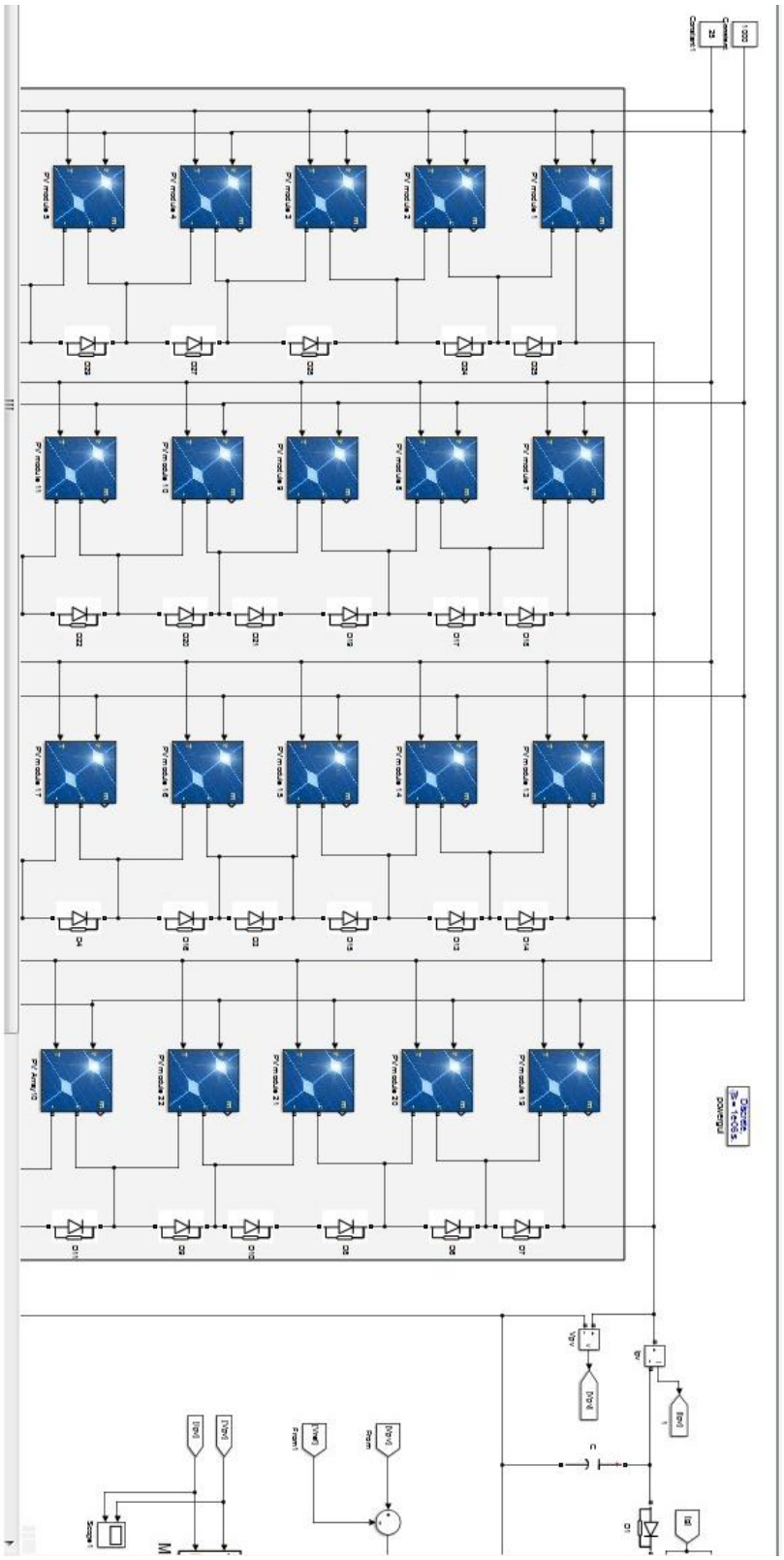

Appendix B

Electrical Characteristics

		290W	295W	300W	305W
Nominal Output (Pmpp)	W	290	295	300	305
Voltage at Pmax (Vmpp)	V	32.0	32.2	32.5	32.7
Current at Pmax (Impp)	A	9.1	9.2	9.2	9.3
Open Circuit Voltage (Voc)	V	39.8	40.1	40.5	40.8
Short Circuit Current (Isc)	A	9.6	9.8	9.9	10.1
Output Tolerance	%	+3/-0			
No. of Cells & Connections		60 in series with 3 bypass diodes			
Cell Type		6" Monocrystalline			
Module Efficiency	%	17.7	18.1	18.4	18.7
Temperature Coefficient of Pmpp	%/C	-0.38			
Temperature Coefficient of Voc	%/C	-0.28			
Temperature Coefficient of Isc	%/C	-0.04			

Mechanical Characteristics

Laminate	Glass: 3.2 high transmission, tempered, anti-reflective Encapsulant: EVA Backsheet: Weatherproof film (black/white)
Frame	Anodized aluminum (Black)
Junction Box	IP68, IEC certified, UL listed
Output Cables	4 mm² (12AWG) cables, Length 1.0m (39.4")
Connectors	Polarized MC4 compatible Weatherproof, IEC certified, UL listed
Weight	19.0 kg (41.9 lbs)

Dimensions

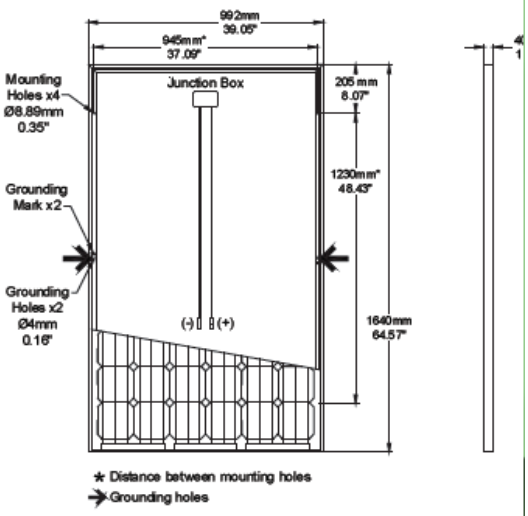

Operating Conditions

Nominal Operating Cell Temperature	46° C + 2
Operating Temperature	-40 to 85° C
Maximum System Voltage	1000v
Maximum Series Fuse Rating	20A
Fire Performance	Type 2
Maximum Wind Load	30 lbs/ft²

SAINT-GOBAIN

CertainTeed Corporation

ROOFING • SIDING • TRIM • DECKING • RAILING • FENCE • GYPSUM • CEILINGS • INSULATION

20 Moores Road Malvern, Pa 19355 Professional: 800-233-8990 Consumer: 800-782-8777 certainteed.com